# NAVAL POSTGRADUATE SCHOOL
# MONTEREY, CALIFORNIA


# THESIS

**ACOUSTIC SOURCE AND DATA ACQUISITION SYSTEM FOR A HELICOPTER ROTOR BLADE-VORTEX INTERACTION(BVI) NOISE REDUCTION EXPERIMENT.**

by

Brian D. Roth

December, 1996

Thesis Advisors: Robert M. Keolian
Steven R.Baker

**Approved for public release; distribution is unlimited.**

# REPORT DOCUMENTATION PAGE

Form Approved OMB No. 0704-0188



| 1. AGENCY USE ONLY *(Leave blank)* | 2. REPORT DATE December 1996 | 3. REPORT TYPE AND DATES COVERED Master's Thesis |
|---|---|---|

4. TITLE AND SUBTITLE ACOUSTIC SOURCE AND DATA ACQUISITION SYSTEM FOR A HELICOPTER ROTOR BLADE-VORTEX INTERACTION(BVI) NOISE REDUCTION EXPERIMENT.

5. FUNDING NUMBERS

6. AUTHOR(S) Brian D. Roth

7. PERFORMING ORGANIZATION NAME(S) AND ADDRESS(ES)
Naval Postgraduate School
Monterey CA 93943-5000

8. PERFORMING ORGANIZATION REPORT NUMBER

9. SPONSORING/MONITORING AGENCY NAME(S) AND ADDRESS(ES)

10. SPONSORING/MONITORING AGENCY REPORT NUMBER

11. SUPPLEMENTARY NOTES The views expressed in this thesis are those of the author and do not reflect the official policy or position of the Department of Defense or the U.S. Government.

12a. DISTRIBUTION/AVAILABILITY STATEMENT
Approved for public release; distribution is unlimited.

12b. DISTRIBUTION CODE

13. ABSTRACT *(maximum 200 words)*

One of the most objectional noises produced by a helicopter is due to interaction of a rotor blade with a previously shed vortex. Various methods have been proposed to reduce this blade-vortex interaction (BVI) noise; this investigation is concerned with BVI noise reduction by rotor blade tip design modifications. Potentially much can be learned regarding the prospect for success of a candidate rotor blade design at greatly reduced time and money by performing acoustic scattering measurements in an anechoic chamber. It is proposed that a rotor blade which scatters acoustic waves less could be expected to produce less BVI noise. This thesis describes the development of the acoustic source and computer controlled data acquisition system for such a scattering experiment.

14. SUBJECT TERMS Blade-Vortex Interaction (BVI), Acoustic scattering measurements, Anechoic chamber, Helicopter noise reduction

15. NUMBER OF PAGES 75

16. PRICE CODE

| 17. SECURITY CLASSIFICATION OF REPORT | 18. SECURITY CLASSIFICATION OF THIS PAGE | 19. SECURITY CLASSIFICATION OF ABSTRACT | 20. LIMITATION OF ABSTRACT |
|---|---|---|---|
| Unclassified | Unclassified | Unclassified | UL |

NSN 7540-01-280-5500

Standard Form 298 (Rev. 2-89)
Prescribed by ANSI Std. 239-18 298-102

**Approved for public release; distribution is unlimited.**

**ACOUSTIC SOURCE AND DATA ACQUISITION SYSTEM FOR A HELICOPTER ROTOR BLADE-VORTEX INTERACTION(BVI) NOISE REDUCTION EXPERIMENT.**

Brian D. Roth
Lieutenant, United States Navy
B.S., Taylor University, 1988

Submitted in partial fulfillment
of the requirements for the degree of

**MASTER OF SCIENCE IN ENGINEERING ACOUSTICS**

from the

**NAVAL POSTGRADUATE SCHOOL**
**December 1996**

Author: Brian D. Roth

Brian D. Roth

Approved by: Robert Keolian

Robert M. Keolian, Thesis Advisor

Steven R Baker

Steven R. Baker, Thesis Advisor

Robert Keolian

Robert M. Keolian, Chairman,
Engineering Acoustics Academic Committee

## ABSTRACT

One of the most objectional noises produced by a helicopter is due to interaction of a rotor blade with a previously shed vortex. Various methods have been proposed to reduce this blade-vortex interaction (BVI) noise; this investigation is concerned with BVI noise reduction by rotor blade tip design modifications. Potentially much can be learned regarding the prospect for success of a candidate rotor blade design at greatly reduced time and money by performing acoustic scattering measurements in an anechoic chamber. It is proposed that a rotor blade which scatters acoustic waves less could be expected to produce less BVI noise. This thesis describes the development of the acoustic source and computer controlled data acquisition system for such a scattering experiment.

## TABLE OF CONTENTS

## LIST OF SYMBOLS

| | |
|---|---|
| $p'(x,t)$ | Far field radiated acoustic pressure |
| $\Delta L$ | Local sectional lift of a blade |
| $M_R$ | Tip mach number of the blade. |
| $c_0$ | Speed of sound in air. |
| R | Distance between source and receiver, $\|\eta - x\|$. |
| r | Radius of the source aperture |
| $\lambda$ | Wavelength |
| f | Frequency |
| x(n) | Input signal |
| y(n) | Output signal |
| h(n) | Impulse response of system |
| $X(\omega)$ | Input signal in frequency domain |
| $Y(\omega)$ | Output signal in frequency domain |
| $H(\omega)$ | System transfer function |
| FFT | Fast fourier transform |
| IFFT | Inverse fast fourier transform |
| $T_{ij}$ | $\rho u_i u_j + P_{ij} - c_0^2 \rho' \delta_{ij}$ |
| $\eta$ | Source position |
| x | Receiver/observer position |
| $\tau$ | Source time |
| dV | Elemental volume in a reference frame fixed to the body |
| dS | Elemental area in a reference frame fixed to the body |
| $\rho'$ | $\rho - \rho_0$ |
| $n_j$ | Unit normal outward from the surface |
| $v_n$ | Velocity of surface in the normal direction |
| $\rho$ | Fluid density |

| | |
|---|---|
| $\rho_0$ | Fluid density at rest |
| $p$ | Fluid pressure |
| $p_0$ | Fluid pressure at rest |
| $\delta_{ij}$ | Kronecker delta |
| $\Omega$ | Revolutions/time of rotor blade |
| $\alpha$ | Angle of attack of rotor blade |
| $U$ | Forward velocity of the aircraft |
| $\zeta$ | Angle between the surface normal in the direction of the force and line from the source to the receiver. |

## ACKNOWLEDGEMENT

The author would first and foremost like to thank God for the salvation he provided through the death and resurrection of his son Jesus Christ to any and every person who is willing to accept his wonderful gift. I would like to thank God for the wonderful blessings he has bestowed on me, my wife Sharice and children, Tyler, Tanyale and T.J. Their unconditional support has always been inspirational. Finally, I would like to thank Professor Steve Baker for the support he provided through necessary equipment and the research vision he had for this project and Professor Robert Keolian for the invaluable guidance he provided in the lab with troubleshooting and programming in LabVIEW.

# I. INTRODUCTION

## A. BACKGROUND AND MOTIVATION

The sound most often associated with a helicopter is the rhythmic, periodic or "wop" sound one hears as a helicopter approaches and flies overhead. It is characteristic of a helicopter and seldom mistaken for anything else. This type of noise is classified as impulsive noise and is annoying to the human ear because of the way the ear processes this type of noise. Who is concerned about this noise and why are they studying it? Those questions can be answered by briefly reviewing the history of helicopter aeroacoustics.

Helicopter noise has been a concern for many years. Research in the area of aeroacoustics for helicopter noise reduction started in the 1950's but tapered off with the development of the jet engine. In the 1960's, the military began using helicopters more frequently and interest in quieter helicopters caused renewed interest in helicopter aeroacoustics. Military interest lies in the area of stealth for attack and rescue helicopters. With quieter military aircraft, both the rescue mission and the attack mission will be more covert, helping to improve the successful completion of those missions. The military is not the only organization interested in this research. Civilian interest has also peaked in the last twenty years, motivated by federal environmental standards for noise. The civilian community would like to use helicopters around populated areas for various information, surveillance, and transportation applications. Due to the current noise level of helicopters, primarily from impulsive noise, civilian use is limited because of the

federal noise level standards. Impulsive noise is severe during descending flight when, the rate of descent of the helicopter matches the rate of descent of the vortices. This may present a public exposure problem during landings, which can often occur in populated areas.

## B. SOURCES OF HELICOPTER NOISE

The sounds produced by a helicopter and their source mechanisms come in a variety of flavors, some which are well understood and others that are not. These noises could be placed into two categories, engine noise and rotor noise, each having subcategories. A helicopter produces both periodic rotor noise at a fundamental frequency and its harmonics, and a broadband noise. The periodic signal results from steady blade forces and blade loading fluctuations and the broadband noise from randomly varying blade forces. During maneuvering or steady flight the periodic noise tends to dominate the spectrum, but during hovering conditions the random signal can become a significant noise source. This research focuses on the periodic noise of blade loading which is called blade-vortex interaction (BVI) noise. BVI noise and high-speed impulsive (HSI) noise are the two most common types of periodic impulsive noise. Each can dominate the noise spectrum. BVI is a serious noise source because, when produced, it dominates the noise spectrum, and, because of its impulsive nature and frequency range, it is annoying to the human ear (George, Helicopter Noise: State of the art).

The reason these impulsive noises are the most objectionable to the ear is due to the way the ear responds to sounds. At large sound levels, the ear automatically increases

the tension of the muscles controlling the ossicles, the small bones of the middle ear. These bones transmit motion from the outer to the inner ear. As the intensity increases, the tensed muscles reduce the amplitude of the motion to prevent damage to the inner ear. The process is called acoustic reflex and it takes about 0.5 milliseconds after the perceived sound for the reflex to occur. Therefore, loud impulsive sounds of short duration do not allow the ear time to adjust and protect itself (Kinsler, Frey, Coppens, and Sanders, pp.258-259, 1982). The frequencies characteristic of BVI noise exacerbate the annoyance of this sound. BVI noise dominates the helicopter noise spectrum in the low to middle frequency range, shown in Figure 1.1.

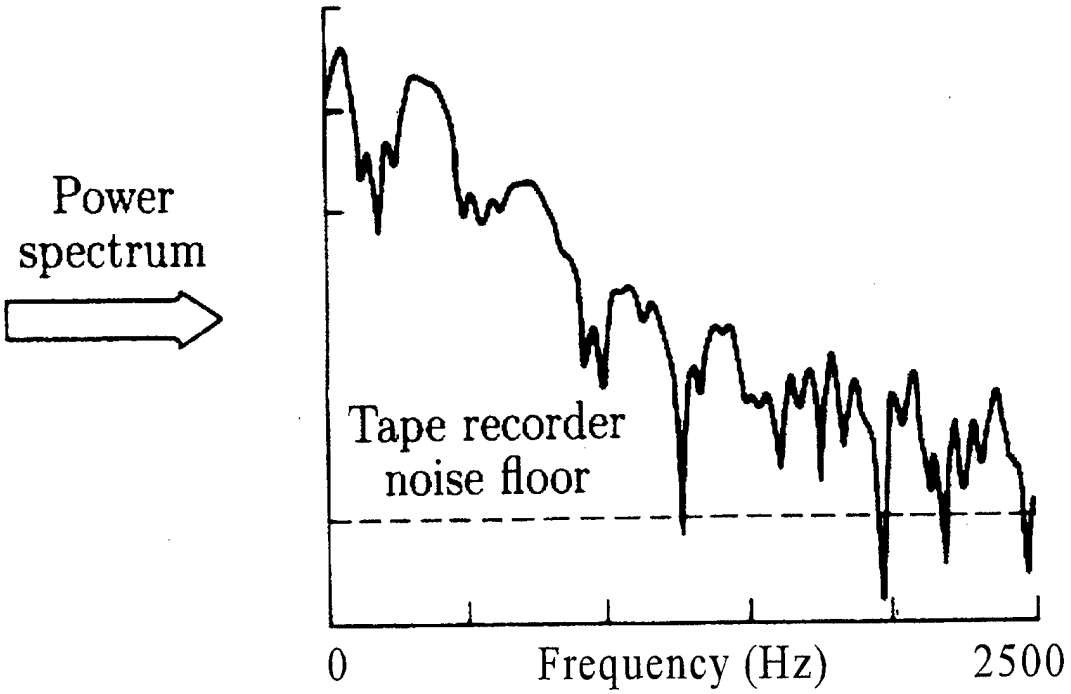


Figure 1.1. Typical BVI spectrum showing that BVI dominates at low frequencies (After Hubbard, p. 103, 1995)

In general, higher frequencies tend to be more annoying to the ear than lower frequencies because of the rapid increase in the hearing sensitivity with increasing frequency (up to about 1 kHz). The hearing threshold is the minimum detectable free-field intensity level of a tone (Kinsler, Frey, Coppens, and Sanders, p. 262, 1982). As the intensity of a sound increases, the acoustic reflex mechanism responds to reduce the movement of the bones in the middle ear. However, as the frequency increases, the acoustic reflex is less efficient and the sound becomes more annoying. Figure 1.2 shows the relationship of frequency to annoyance level and Figure 1.3 shows how sound is attenuated by the atmosphere (George, Helicopter Noise: State of the art). It is evident that higher frequencies are more annoying, but also have significant attenuation. Figures 1.2 and 1.3 combined show that frequencies above 2000 Hz propagating through the atmosphere are not very significant when considering annoyance to the human ear. BVI noise tends to be strongest between 500 and 2000 Hz, impulsive in nature, and amplified during descending flight. The combination of these three factors makes BVI noise a very annoying source of helicopter noise and the need for continued improvements in rotor blade designs to reduce this phenomena becomes evident.

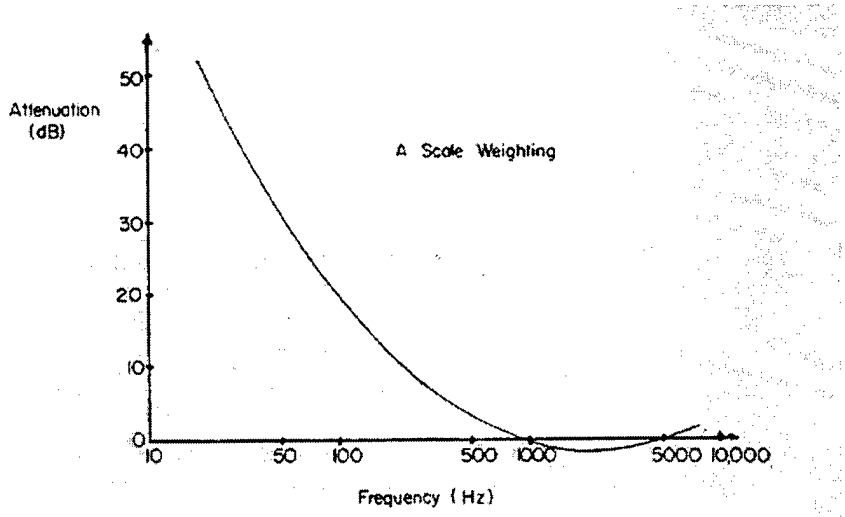


Figure 1.2. Weighted Sound levels for the human ear measuring levels of annoyance in dB versus frequency (George, p.707, 1978)

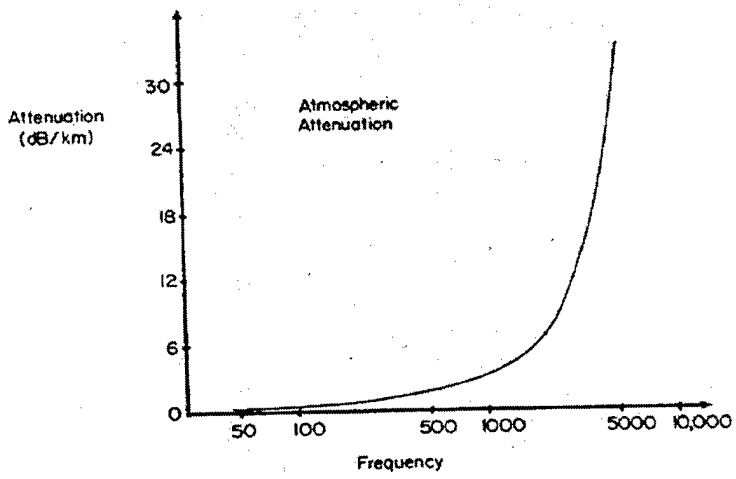


Figure 1.3. Attenuation of sound in quiescent atmosphere (dB per kilometer)at 20 C, 50% relative humidity (George, p.709, 1978)

## C. SOLUTIONS TO THE HELICOPTER NOISE PROBLEM

Many solutions to the problem of BVI noise have been proposed and attempted, with varying degrees of success. Varying the tip design of the rotor blades, individual blade control (IBC), and higher harmonic control (HHC) are a few of the more popular ideas to control BVI noise. Figure 1.4 shows some blade tip designs. The problem is twofold. First we must understand the source mechanism of the noise so we can better model and predict the noise to assist in blade design techniques and secondly, develop solutions that fix the BVI noise problem but do not enhance another, which is happening in many of the current design initiatives.

Understanding the source is still an unsolved problem. Many modeling projects are underway and definite progress is apparent, but none can reproduce the BVI event

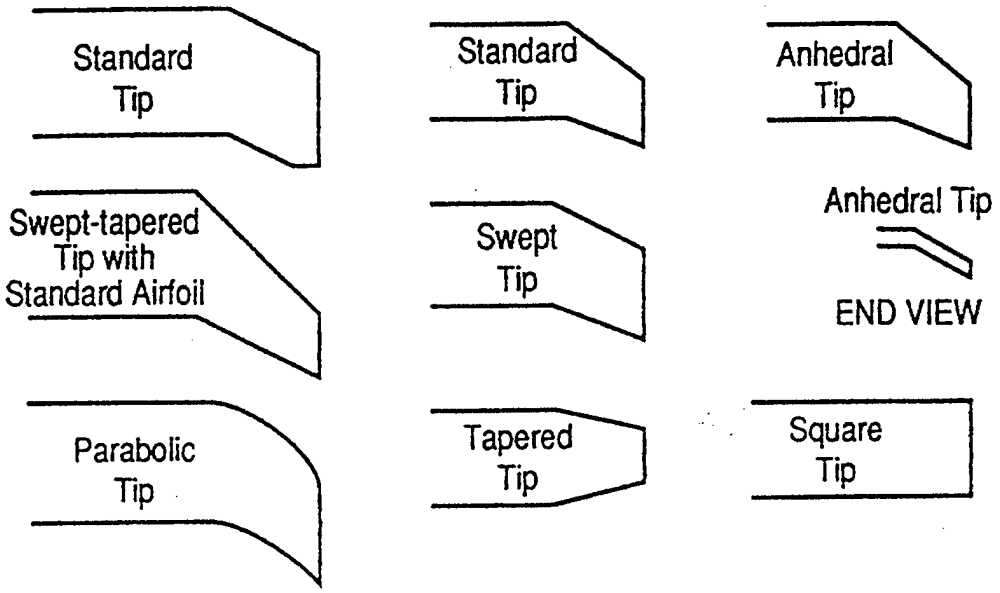


Figure 1.4. Various blade designs used to reduce BVI (After Brooks, p.62, 1993)

under all circumstances consistently. A reduction of 6 dB has been observed with HHC, an active feedback technique, but it also has enhanced BVI under some situations (Brooks, p. 58, 1993). Therefore, the solution has no silver bullet. Many ideas will have to be fused together in order to develop an acceptable solution.

## D. SCOPE

In the present investigation, BVI noise reduction by rotor blade tip design modifications is being pursued using a unique method employing acoustic scattering measurements on a stationary blade in an anechoic chamber. This thesis describes the development of the acoustic source and computer-controlled data acquisition system for the experiment. The idea is to impinge an acoustic wave that matches that encountered during a BVI event and measure the scattered acoustic field. It is proposed that a rotor blade which scatters acoustic waves less could be expected to produce less BVI noise. Although it is not possible to duplicate flight conditions exactly in an anechoic chamber, as a proof-of-principle method, stationary anechoic chamber testing has many advantages. It is low-cost, safe, modifications are easy to make, and one can focus on the acoustics of the blade because it does not have to withstand the great stresses encountered while spinning.

The remainder of this thesis is organized as follows: Chapter II describes the theory and production mechanisms of blade-vortex interactions (BVI).

Chapter III describes the source and data acquisition system, and includes a discussion of the acoustic scattering experiment and signal processing concepts necessary to duplicate the BVI pressure pulse. The experimental results for the source electrical-to-acoustic transfer function, generated voltage waveform, and duplicated BVI pressure pulse are also presented

Chapter IV includes conclusions and recommendations for continued research into the scattering measurements of the BVI signal.

## II. THEORY OF BLADE-VORTEX INTERACTION(BVI) NOISE

BVI is the interaction between a blade and a previously shed vortex. The vortices are produced at the blade tips as the air passes from a high pressure region to a low pressure region, or from the bottom of the blade to the top (El-Ghobashy, 1996). These vortices spin in a whirlwind fashion leaving a spinning trail of air behind the blade tip. Due to the location and strength of the shed vortex, the induced velocity felt by the blade varies. This variation in induced velocity causes a variation in the blade angle of attack and therefore the instantaneous lift of the blade changes (Sim and George, 1995, p. 526). It is the change in lift, or 'loading' on the blade, that causes the impulsive noise to be radiated and the impulsive nature is what disturbs the human ear. At high advancing tip speeds, the strength of the BVI event is primarily determined by the mach number of the blade tip and thickness of the blade (Brooks, p.57, 1993). However, simply reducing the tip mach number or the thickness of the blade has not reduced the strength of the vortex to such a level that BVI events become insignificant. Additionally, there are other parameters such as lift that have to be considered when changing the tip mach number. At lower tip speeds, the complexity of the problem increases because more parameters become important.

In order to discuss the various factors that make this phenomenon so difficult to model, one must understand how sound is radiated from a body in arbitrary motion and then investigate simplifications that will help evaluate expected radiated noise in the far field.

Equation 2.1 governs the noise generated by a body in arbitrary motion, where $c_0$ is the speed of sound, $T_{ij}$ are the quadrupole sources, $P_{ij}n_j$ is the force per unit area exerted on the fluid by the surface of the body, x is the observer position, $\eta$ is the source position, R is the distance between source and observer, t is the observer time, $M_R$ is the mach number in direction of the observer, $\tau$ is the source time, dV is the elemental volume in a reference frame fixed to the body, dS is the elemental area in a reference frame fixed to the body, $\rho'$ is the difference in fluid pressure densities, $\rho_0$ is the fluid pressure at rest and $v_n$ is the velocity of a surface in the normal direction (Hubbard, pp. 69-70, 1995). The left hand side of the equation is the acoustic pressure and the hand right side can be broken into three distinct terms. The first term is the noise due to fluid stress, the second is the noise due to blade surface pressure pushing on the fluid, and the final term is the noise due to the blade displacing fluid as it traverses its circular path (Hubbard, p. 71, 1995).

$$\pi c_o^2 \rho'(x,t) = \frac{\partial^2}{\partial x_i \partial x_j} \iiint \left[\frac{T_{ij}}{R|1-M_R|}\right]_\tau dV(\eta) - \frac{\partial}{\partial x_i} \iint \left[\frac{P_{ij} n_{ij}}{R|1-M_R|}\right]_\tau dS(\eta) + \frac{\partial}{\partial t} \iint \left[\frac{\rho_0 v_n}{R|1-M_R|}\right]_\tau dS(\eta) \qquad 2.1$$

This equation first appeared in a paper in 1969 and is a direct extension of Lighthill's aerodynamic sound theory. Since equation 2.1 is an exact equation, some simplification is necessary to develop a workable theory. The first assumption is that the rotor blades are thin, which allows linearization of the flow equations. The first term on the right hand side contains the quadrupole sources $T_{ij}$. Due to linearization and the fact that the quarupole sources only contain second order perturbations, the first term can be neglected, leaving only the second and third terms. The second assumption is that only steady forces, those forces not varying over time, are significant. The justification for this is based on the idea that steady sources moving supersonically have a greater source strength than unsteady forces. Therefore, $P_{ij}n_j$ simplifies to representing only the steady forces. BVI noise is a force or blade loading noise which is the result of the second term of equation 2.1, equation 2.2. (Hawkings and Lawson, pp. 2-7, 1974)

$$\frac{\partial}{\partial x_i}\int\int[\frac{P_{ij}n_j}{R|1-M_R|}]_\tau dS(\eta) \qquad 2.2$$

Although equation 2.1 was simplified somewhat, equation 2.2 needs to be further reduced to understand the specific parameters that are significant in the production of BVI noise. In order to simplify equation 2.2, the entire blade will be treated as a single radiating body and the receiver will be assumed to be in the far field. With these assumptions and the relationship given in equation 2.3, the simplified acoustic pressure

radiated by a BVI event is given by equation 2.4, where ΔL is the local sectional lift of a blade, ζ is the angle between the surface normal in the direction of the force on the fluid and a line from the point of the applied force to the observer, and n is the normal vector in the direction of the applied force.

$$P_{ij}n_j \approx \Delta L\bar{n}\bullet\bar{R} = \Delta L\cos\zeta \qquad 2.3$$

$$p'(x,t)=\frac{1}{4\pi}\frac{\partial}{\partial t}\frac{1}{c_0}\left[\frac{\Delta L\cos\zeta}{R|1-M_R|}\right]_\tau \qquad 2.4$$

Figure 2.1 shows the geometry used in developing the relationship in equation 2.3. (Hubbard, pp. 86-87, 1995)

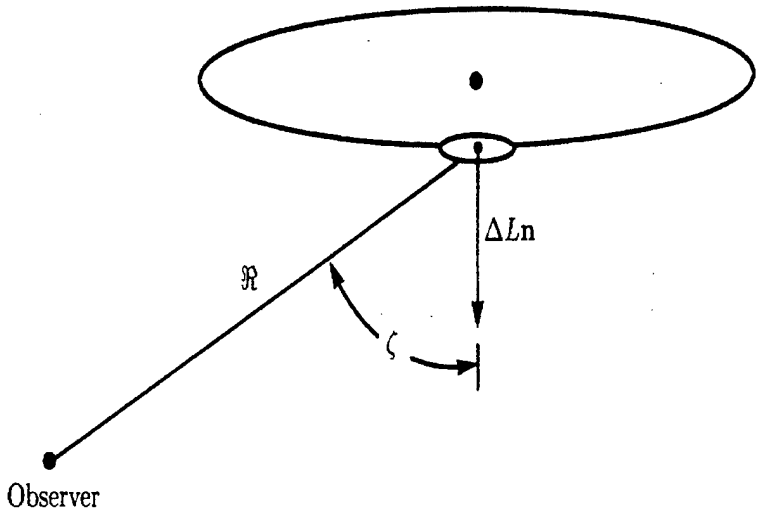


Figure 2.1. Geometry for far field observer (Hubbard, p. 87, 1995)

Equation 2.4 illustrates that the resulting pressure field is primarily dependent on four factors: local sectional lift of a blade, $\Delta L$, the angle between the normal direction of force and the observer, $\zeta$, the range to the observer, R, and the doppler factor ,1- $M_{R,}$ which results from using the moving-blade frame of reference. Two other factors, lift time history and the geometry between the shed vortex and the approaching blade, play an important role as well.

BVI event geometry is probably the most important factor because if the blade and a previously shed vortex do not encounter each other, this discussion is "pointless". Experimental evidence suggests that the outer 20 to 30 percent of the blade needs to pass close to a shed vortex in order for an unwanted acoustic pressure field to radiate (Hubbard p. 82, 1995). This generally occurs during descending flight due to the upflow of air pushing the shed vortices into the blade plane. Figure 2.2 shows both steady and descending flight.

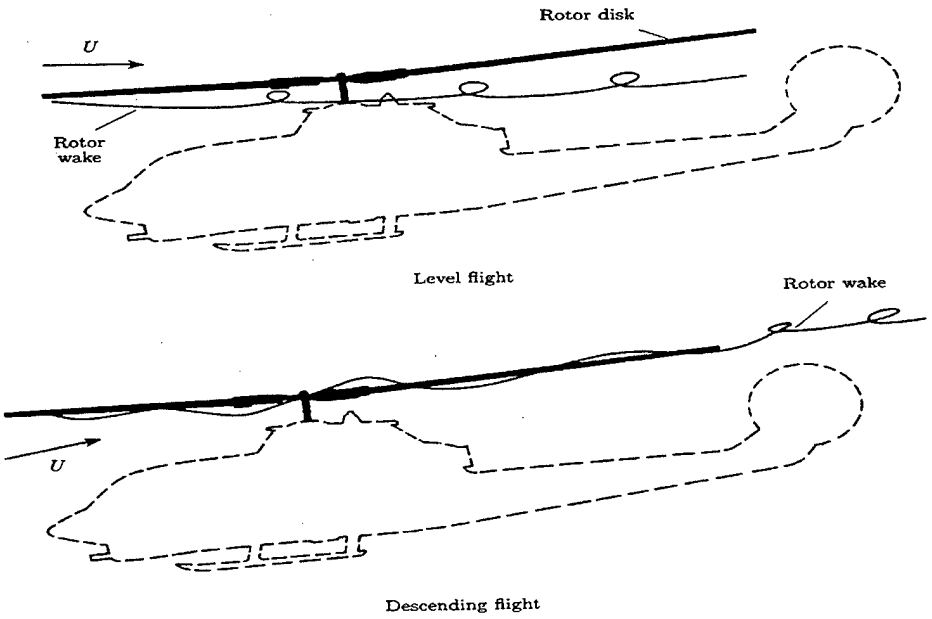


Figure 2.2. BVI geometry for steady and descending flight (Hubbard, p.85, 1995)

The bottom picture of Figure 2.2 graphically shows the shed vortices encountering a blade during descending flight. The reason this amplifies the BVI problem is that descending flight usually occurs near populated areas, where noise reduction is desired. Figure 2.3 is an expanded view of BVI events during a partial descent. It shows seven possible interaction points. Interaction three is especially important because the vortex and blade are essentially parallel during the interaction, the situation which generally radiates the strongest acoustic energy.

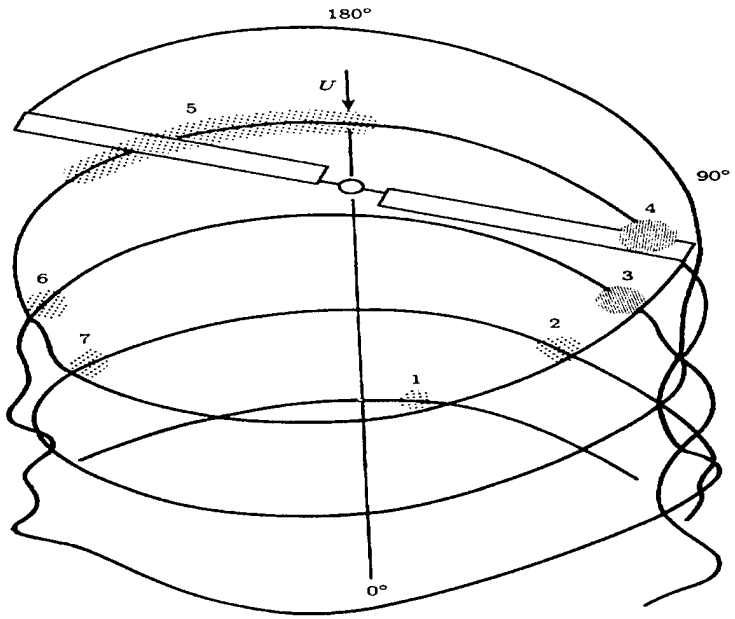


Figure 2.3. BVI interactions during descending maneuver.

(Hubbard, p.84, 1995)

Tip mach number, or doppler factor, is another factor that affects the severity of the radiated noise. As can be seen in equation 2.4, as tip mach number increases toward 1, the denominator gets smaller and the overall effect is a larger radiated pressure field. Further analysis needs to be done when mach number approaches one because a singularity exists in equation 2.4.

When designing a blade and determining the tip mach number necessary, there are other factors besides BVI noise to consider, such as rotor thrust, flight conditions, tip shape, twist, number of blades, and rotor speed (Brooks, 1993). However, newer blade designs have reduced tip mach numbers from the range 0.8-0.9 to 0.5-0.6 during steady flight.

BVI noise has been observed to have significant directivity. In fact, one of the early solutions to reducing BVI noise was having the pilot fly in such a manner that no BVI noise was heard in the aircraft. However, as more research became available, the directional nature of BVI noise showed that strong acoustic fields were radiated to the ground even when the pilot could not hear the event in the aircraft. Figure 2.4 shows the longitudinal directivity of BVI and suggest that angles between 10 and 45 degrees are the most severe. The negative angles shown or angles near 0 are not as important because that noise is not radiated toward the ground.

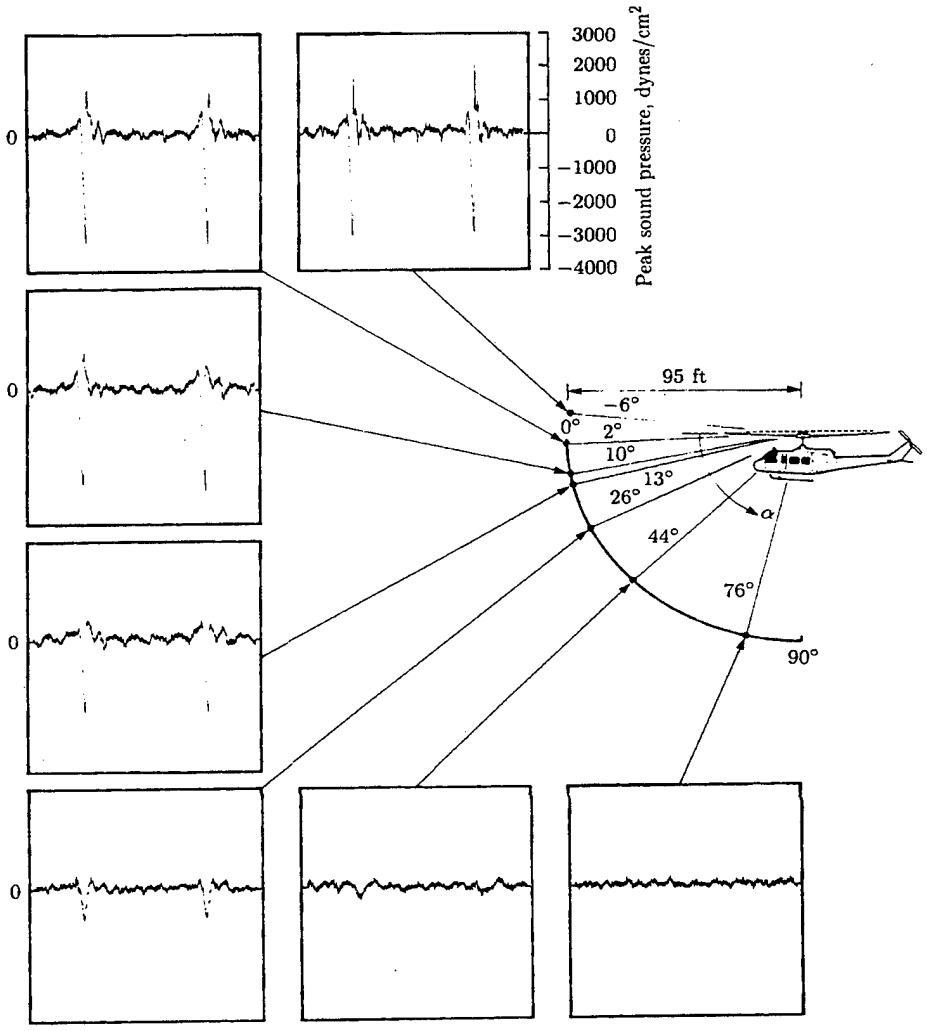


Figure 2.4. Longitudinal directivity for level flight (Hubbard, p. 97, 1995)

Figure 2.5 shows the lateral directivity and indicates that directly in front of the helicopter is where the strongest BVI noise was measured. Therefore, the directional nature of BVI is significant and suggest that an observer directly in the flight path at an

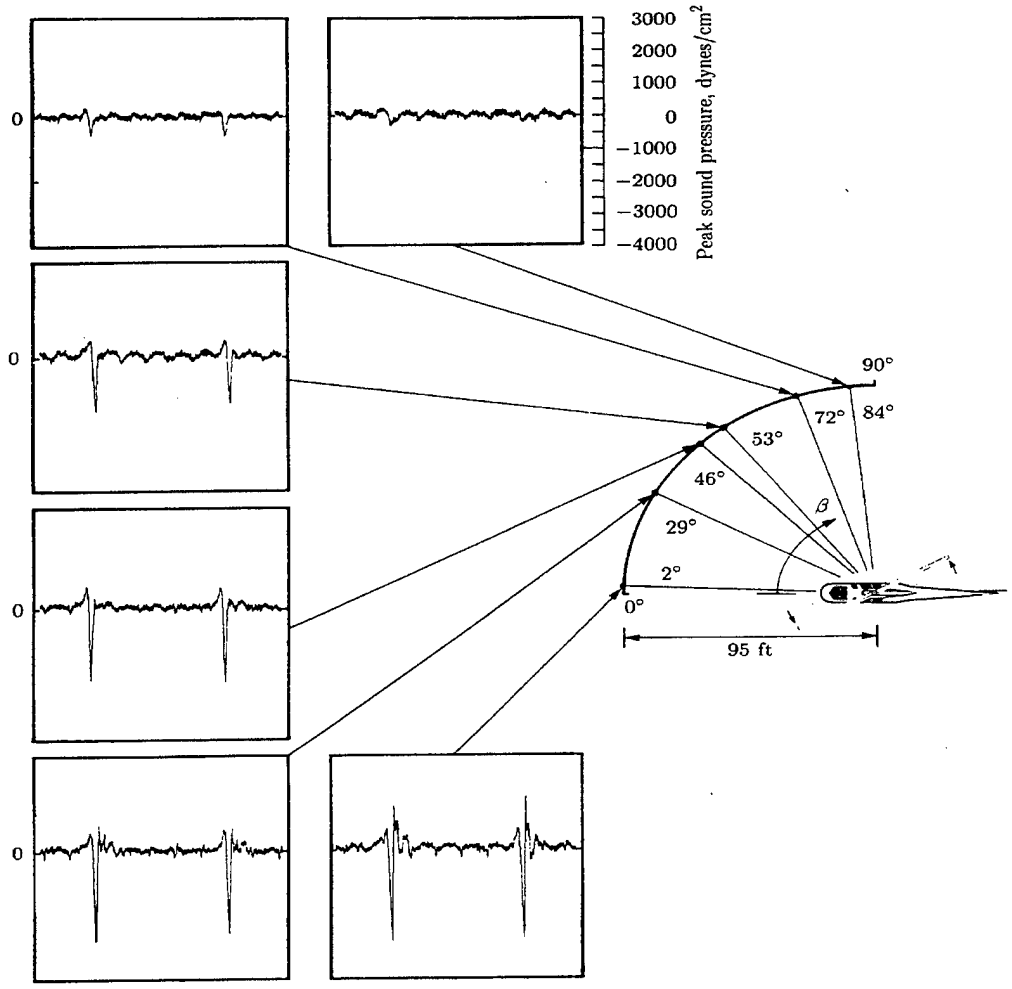


Figure 2.5. Lateral acoustic directivity for level flight (Hubbard, p. 98, 1995)

angle $\alpha$ of 10 to 45 degrees will hear the strongest radiated pressure field due to a BVI event. Figure 2.6 shows how the measurements were performed.

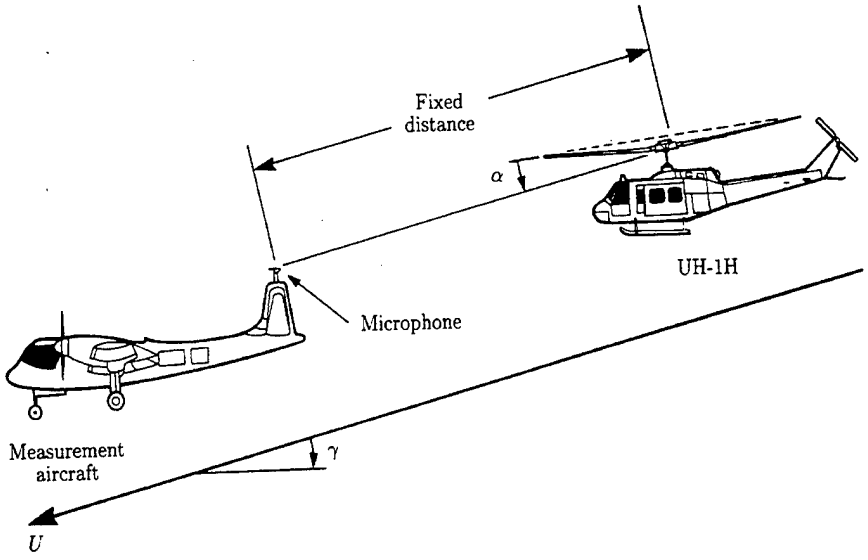


Figure 2.6. Flight geometry for measurements in Figures 2.5 and 2.6.

(Hubbard, p. 85, 1995)

The final parameter is the lift, ΔL, of the blade. Encounter three of Figure 2.3 will be used to discuss the expected change in lift time history due to the change in angle of attack of the blade during a BVI event. Because the vortex and blade are parallel during the encounter, the BVI event reduces to a two dimensional problem. Figures 2.7 shows a possible angle of attack time history for the advancing side BVI event. Using equation 2.5, Figure 2.8 shows the resulting lift time history, assuming incompressible flow.

$$\Delta L \propto \Omega R + U\sin\alpha, \qquad 2.5$$

where Ω is the blade rotational frequency, U is the forward velocity of the helicopter, α is the angle of attack of the rotor blade, and R is the radius of the rotor blade.

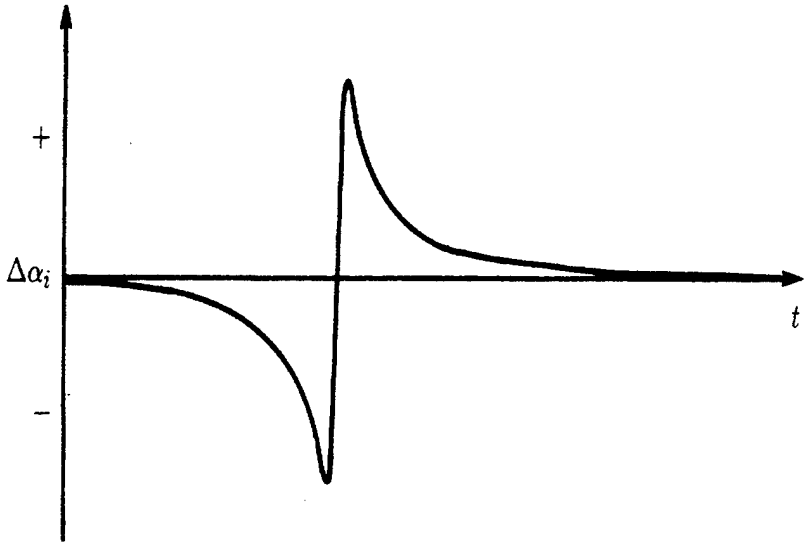


Figure 2.7. Possible angle of attack time history for parallel BVI event

(Hubbard, p. 86, 1995)

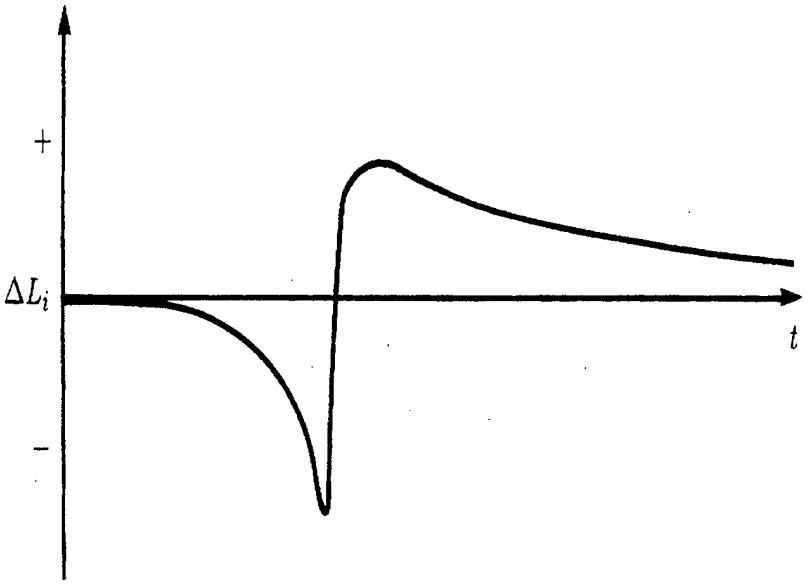


Figure 2.8. Lift time history due to angle of attack in Figure 2.7

(Hubbard, p. 86, 1995)

Figure 2.9 shows the resulting BVI acoustic pressure field for the simple geometry of the vortex and blade parallel during the interaction.

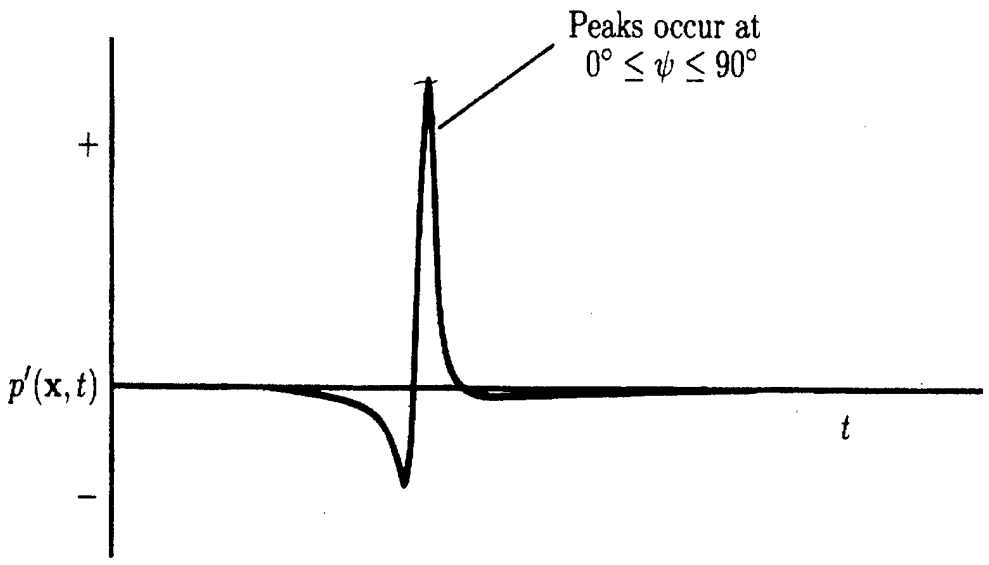


Figure 2.9. Typical acoustic pressure pulse of a BVI event (Hubbard, p.87, 1995)

# III. ACOUSTIC SOURCE AND DATA ACQUISITION SYSTEM

## A. DESCRIPTION OF ACOUSTIC SCATTERING EXPERIMENT

Figure 3.1 shows a diagram of the setup for the acoustic scattering experiment for studying BVI noise reduction concepts. The experiment is to be performed in the anechoic chamber. An acoustic source will be excited by a signal generated by the computer-controlled data acquisition system so as to produce a pressure waveform on the surface of the rotor blade section which closely resembles that of a BVI event, (Figure 2.9). The resulting scattered pressure field will be measured. The model rotor blade used for this experiment is made of wood with a blade length of 5 feet and chord length of 6 3/4 inches. The blade it is modeling has a blade tip speed of 500 - 600 feet per second which yields a tip mach speed of between 0.444 and 0.533. The results of acoustic scattering measurements made on this blade and on blades with various passive acoustic treatments, e.g. embedded Helmholtz resonators, will be compared and the value of such treatments in reducing BVI noise will be assessed. The source and data acquisition system, which are the subjects of this thesis, are described in detail below.

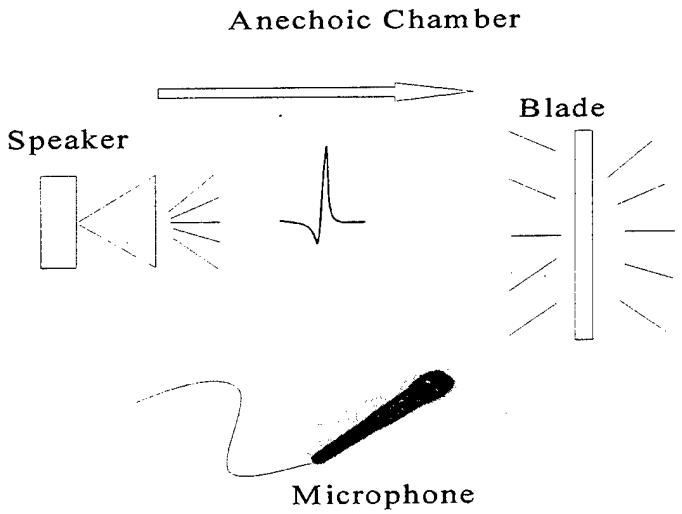


Figure 3.1. Acoustic scattering experiment setup

## B. ACOUSTIC SOURCE

The source is a line array of 1-½ inch diameter soft dome midrange Pioneer speakers with a design frequency response of 1.2 khz - 15 kHz (Pioneer Electronic Corporation, 1996). The data sheet for the speaker can be found in Appendix C. A loudspeaker with a relatively flat frequency range of 1 to 10 kHz was chosen to be able to faithfully reproduce a BVI pressure pulse of approximately 1 ms duration. Figure 3.2 shows the frequency response curve of a single speaker measured in the NPS anechoic chamber. The array consists of 4 segments each 3 feet in length. Each 3 foot section contains 8 speakers wired such that the overall impedance is twice the impedance of a single speaker (6.5 ohms). Two of these sections can be used together to form a six foot

array and the two six foot arrays can be placed side by side to form a larger array. The source can be used as either a monopole source or a dipole source.

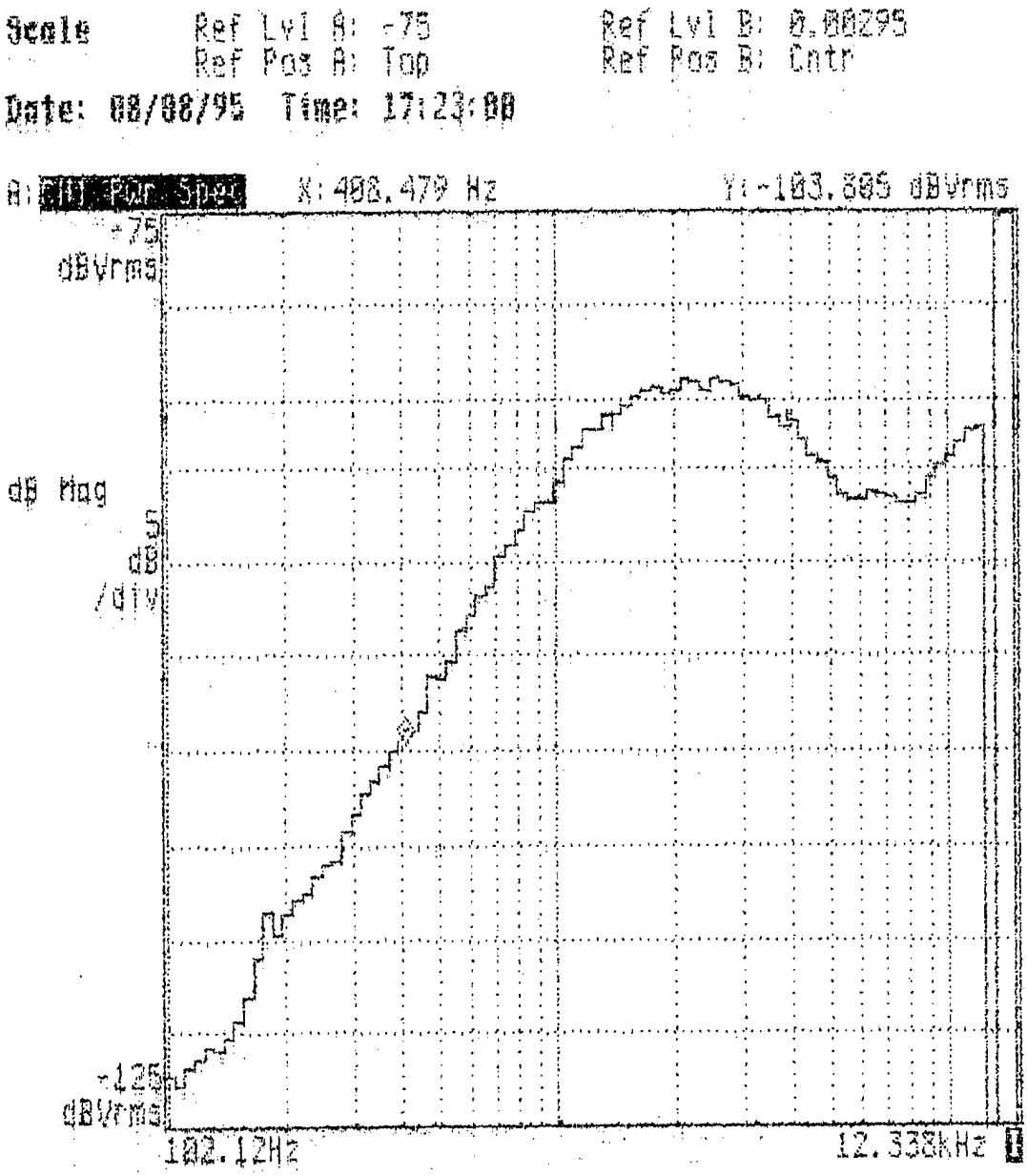


Figure 3.2. Frequency response of a single speaker.

Figure 3.3 shows a photograph of the two arrays and the model rotor blade in the NPS anechoic chamber.

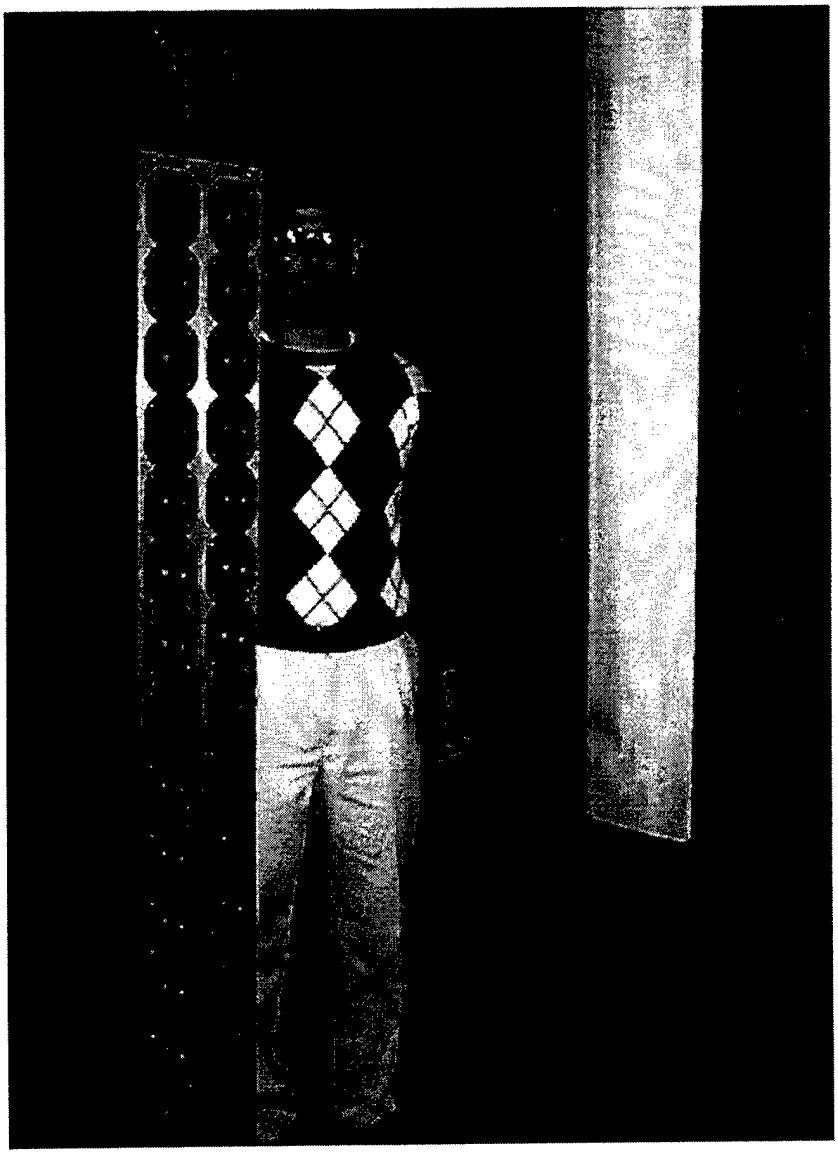

Figure 3.3. Photograph of the two arrays and model rotor blade in the NPS anechoic chamber.

## C. DATA ACQUISITION SYSTEM

The data acquisition system needs to perform the following tasks: (1) develop the transfer function from the electrical stimulus applied to the source and the resulting acoustic response signal from a microphone located at the leading edge of the rotor blade, (2) from this, determine the necessary voltage waveform to be applied to the source to produce an incident pressure waveform at the rotor blade to simulate a BV event and apply this to the source, and (3) collect acoustic scattering data from a second moveable microphone. Figure 3.4 shows a block diagram of the data acquisition system. It is based upon the use of the LabVIEW graphical programming system for computer-control of instrumentation (National Instruments, 1996). A National Instruments NB-A2100 data acquisition card (DAQ) was used in a Macintosh Quadra 800 (with a 60 MHZ Power PC accelerator card) for this purpose. The NB-A2100 contains two 16-bit input and output channels; its specifications are given in Appendix A.

Two separate virtual instruments (VI) were written in LabVIEW 4.01 to accomplish the tasks required of the data acquisition system. The first VI determines the system transfer function and the second VI calculates the required voltage waveform and sends this to the speaker and receives the desired BVI pressure pulse and scattered waves. Simultaneously conducting input and output operations has not been successfully accomplished at this point in this research project, requiring the duplicated BVI pressure pulse to be viewed on an oscilloscope. This problem is discussed in detail later in this chapter.

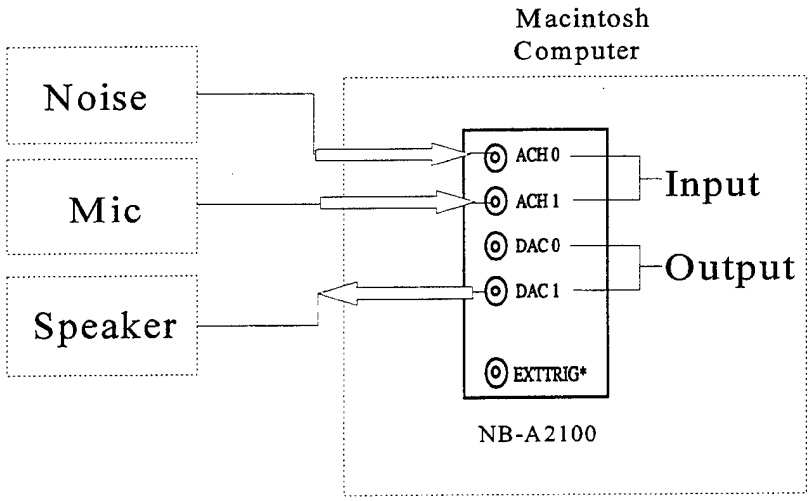


Figure 3.4. Block diagram of the data acquisition system controlled by LabVIEW

## 1. SOURCE SIGNAL PROCESSING

Signal processing is required to generate the desired BVI pressure signal at the blade. The concepts used to accomplish this are described below. Figure 3.5 shows a simple generic system diagram. The input sequence x(n) is transformed by "box" h(n) and produces the output sequence y(n). In the present application, x(n) represents a guassian electrical noise source to be applied to the acoustic source, y(n) the response signal from a microphone located at the leading edge of the rotor blade, and h(n) the "system" impulse response (all sequences are assumed uniformly spaced in time). Equation 3.1 represents the mathematical formulation of Figure 3.5 and becomes much

simpler in the frequency domain. By using the properties of the Fourier Transform, the right side of equation 3.1 becomes a product in the frequency domain instead of a convolution in the time domain, equation 3.2. Solving for the input voltage yields equation 3.3.

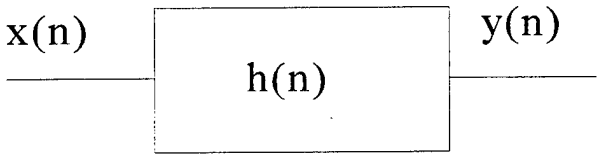


Figure 3.5. Simple system diagram

$$y(n)=x(n)*h(n)=\sum_{k=-\infty}^{\infty} x(k)h(n-k) \qquad 3.1$$

$$Y(\omega)=H(\omega)X(\omega) \qquad 3.2$$

$$x(n)=FFT^{-1}[\frac{Y(\omega)}{H(\omega)}] \qquad 3.3$$

To develop the transfer function it is necessary to provide a stimulus signal x(n). A Guassian noise source will be used as this stimulus signal. By radiating this noise across the blade, the impulse response can be calculated since the stimulus and response signals are both available, the response signal being the output voltage of the microphone, y(n), and the stimulus signal the random noise voltage into the speaker, x(n). By taking the Fourier transform of the impulse response, the transfer function can be determined for a specific experimental situation. Data must be collected for several runs and the average transfer function calculated to eliminate any noise. It is important to note that if any acoustic parameters change, such as the position of the microphone, speaker or blade, or the temperature of the air, the transfer function will need to be reevaluated although it will not change dramatically because the transfer function is dominated by the frequency response of the speaker. With the desired signal and the transfer function known, the pre-distorted input signal to the speaker can be determined. This signal is radiated by the speaker and since the system transfer function is known, the resulting pressure at the microphone is the desired BVI pressure signal.

## 2. SOURCE EXPERIMENT DESCRIPTION AND RESULTS

An experiment was setup to measure the source electrical-to-acoustic transfer function and to use this information to generate the desired BVI pressure signature at the blade, as described in the previous section. This was accomplished by using numerous pieces of equipment and a software package from National Instruments called LabVIEW 4.01. A description of all the equipment is contained in appendices A through C, a description and drawing of the anechoic chamber where the measurements were taken in

appendix D, and the computer code in appendix E. The theory behind how to generate the BVI pulse was given previously, but the specific mechanics of how it was accomplished will be explained here and the results presented.

Figure 3.6 shows a block diagram of the setup for determining the system transfer function. The experiment was performed in an anechoic chamber to eliminate unwanted reflections and noise. The model rotor blade is made of wood with a blade length of 5 feet. The blade it is modeling has a blade tip speed of 500 - 600 feet per second which yields a tip mach speed of between 0.444 and 0.533. The chord length is 6 3/4 inches. The model rotor blade was hung vertically with the leading edge of the blade facing the speaker in the anechoic chamber with a microphone hung very close to the leading edge in the middle of the blade. The blade and sound source were 1 ½ feet or 0.4572 meters apart and the acoustic source (a single speaker) was place at approximately the same height as the microphone.

Guassian noise generated by a synthesized function generator was sent to analog input channel zero of the data acquisition board (DAQ) and to the speaker (through an amplifier). The time domain response of the microphone was amplified and sent to analog input channel 1 of the DAQ board. Once the two signals were digitized, the instantaneous impulse response and transfer function, magnitude and phase, along with the average transfer function were determined. The data were collected and averaged until the average transfer function converged to an acceptable level. This was determined by viewing the graph of the average transfer function. The resulting transfer function was split into real and imaginary parts and then sent to a file to be used in generating the pre-

distorted BVI signal. Appendix H shows a picture of the front panel and diagram of the virtual instrument (VI) used to produce the transfer function along with a description of how the VI works and information on the various components. Figures 3.7 and 3.8 show the magnitude and phase of the measured average transfer function.

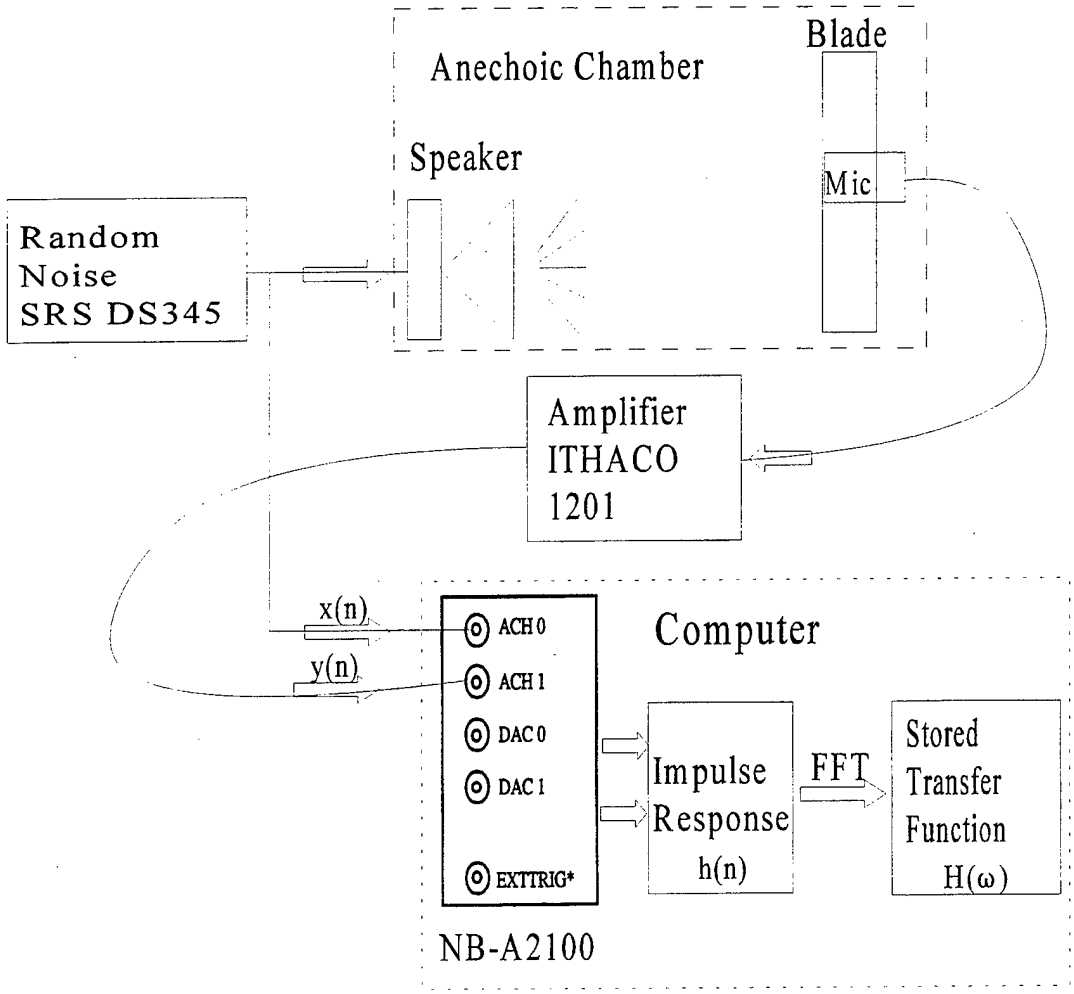


Figure 3.6 Block diagram of determination of system transfer function.

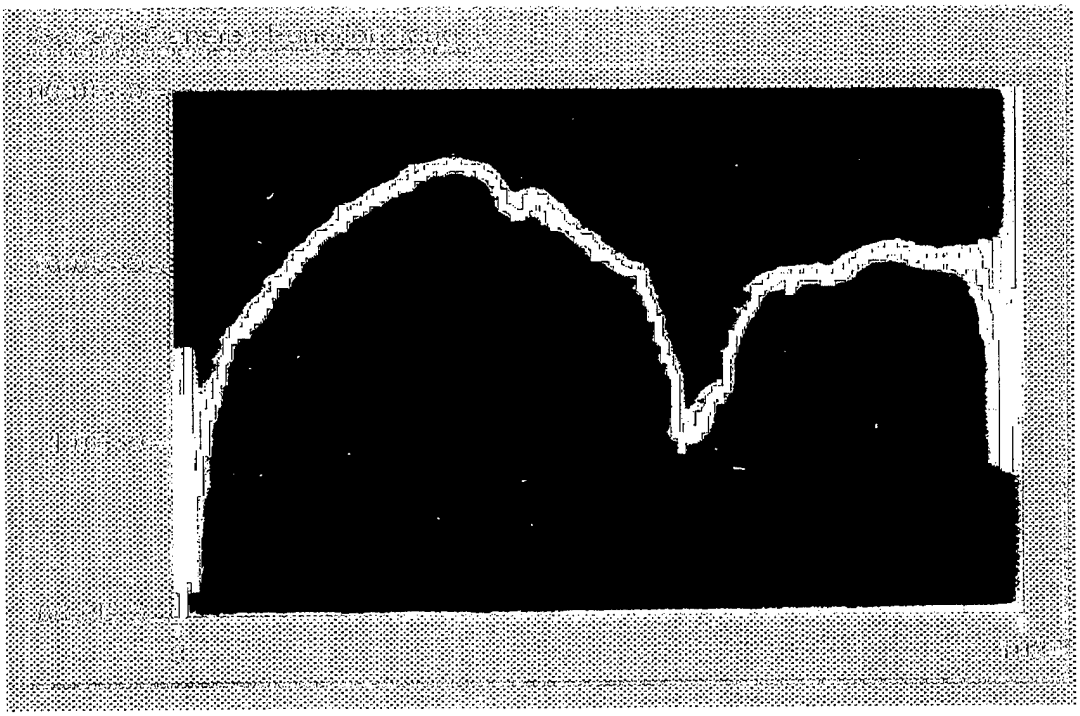

Figure 3.7. Magnitude of the average transfer function.

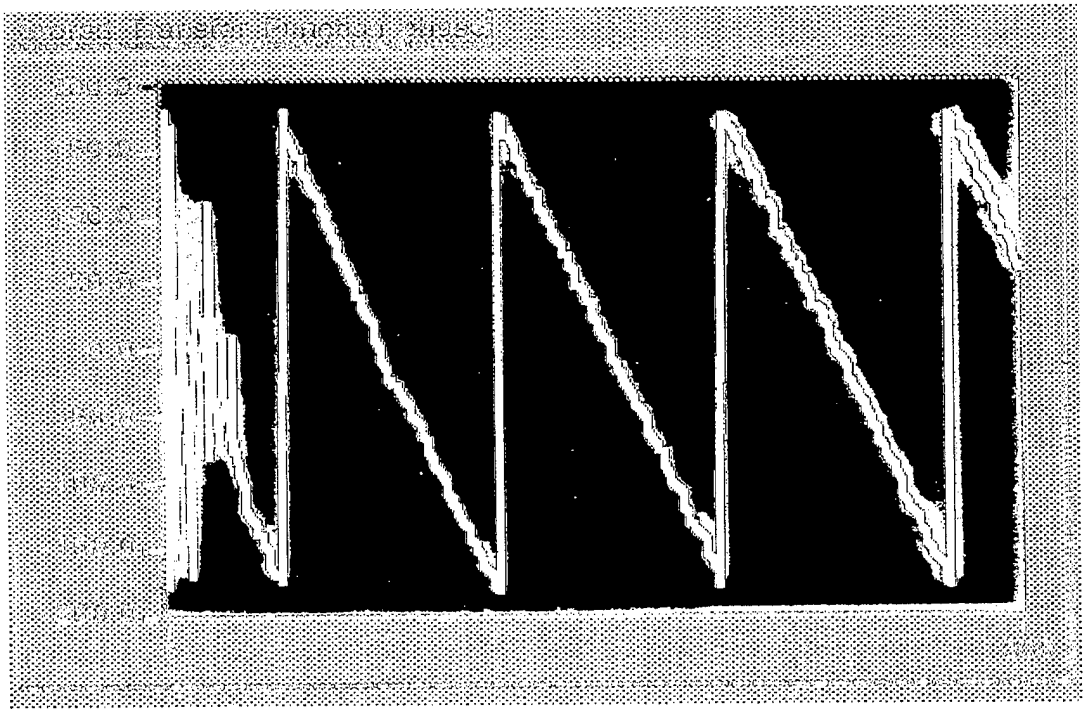

Figure 3.8. Phase of the average transfer function

The block diagram for the system for generating the desired BVI waveform at the rotor blade is shown in figure 3.9.

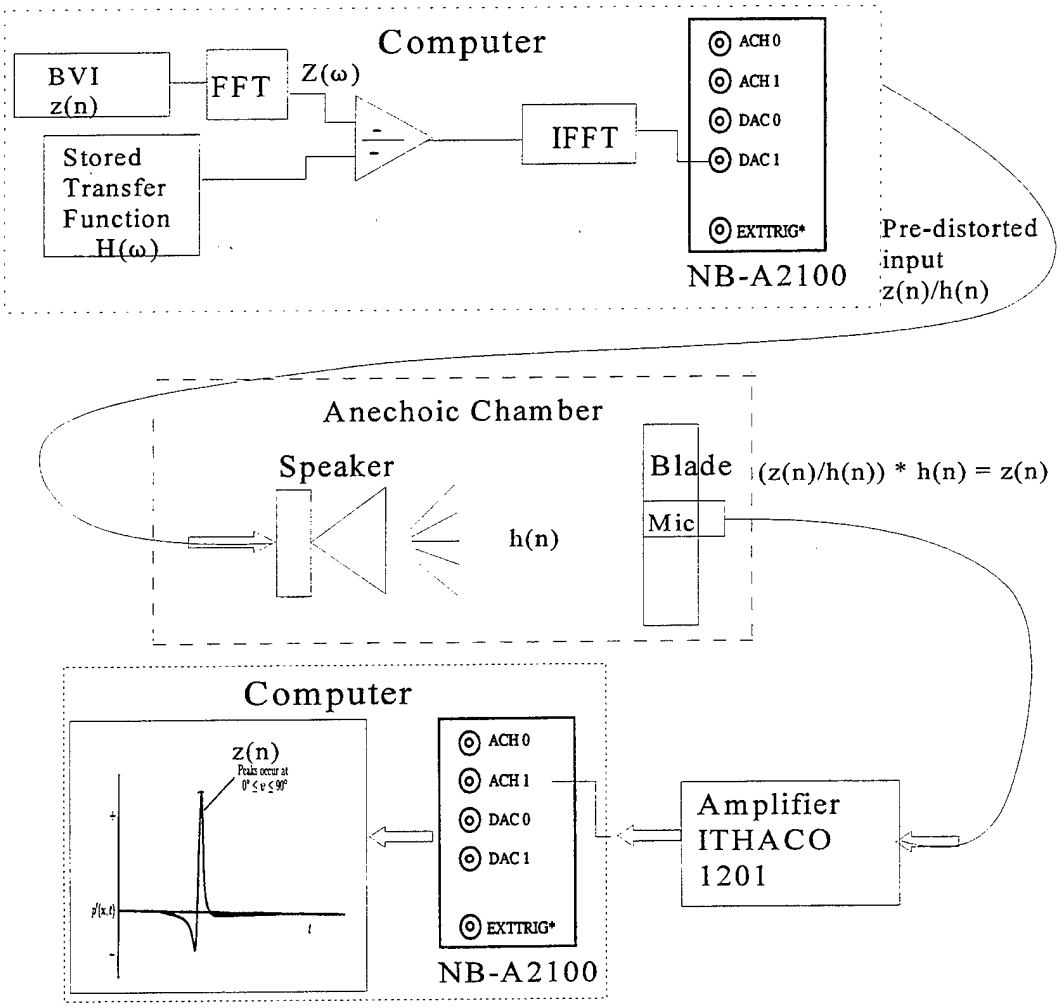


Figure 3.9. Block diagram for duplication of BVI waveform.

The transfer function was retrieved from a file and the real and imaginary parts converted back to a complex number. The desired BVI signal was also retrieved from a file and transformed into the frequency domain. The BVI signal was then divided by the transfer function, the result was transformed back to the time domain and the desired voltage waveform was generated (Figure 3.10). This voltage was sent to the speaker and the desired BVI signal received by the microphone. Figure 3.11 shows a photograph of the desired BVI signal displayed on an oscilloscope. Much difficulty was encountered when the desired BVI signal was digitized by the DAQ board. These problems are discussed at the end of this chapter. 2048 points of data were collected during each scan and the sampling frequency was 22.05 kHz. Since the BVI signal falls primary in the low to middle frequency ranges, 500 - 2000 Hz, assuming a max frequency of 8 kHz allowed the requirements of the Nyquist sampling frequency and allowable sampling frequencies of the NB-A2100 DAQ board to be met and prevented aliasing.

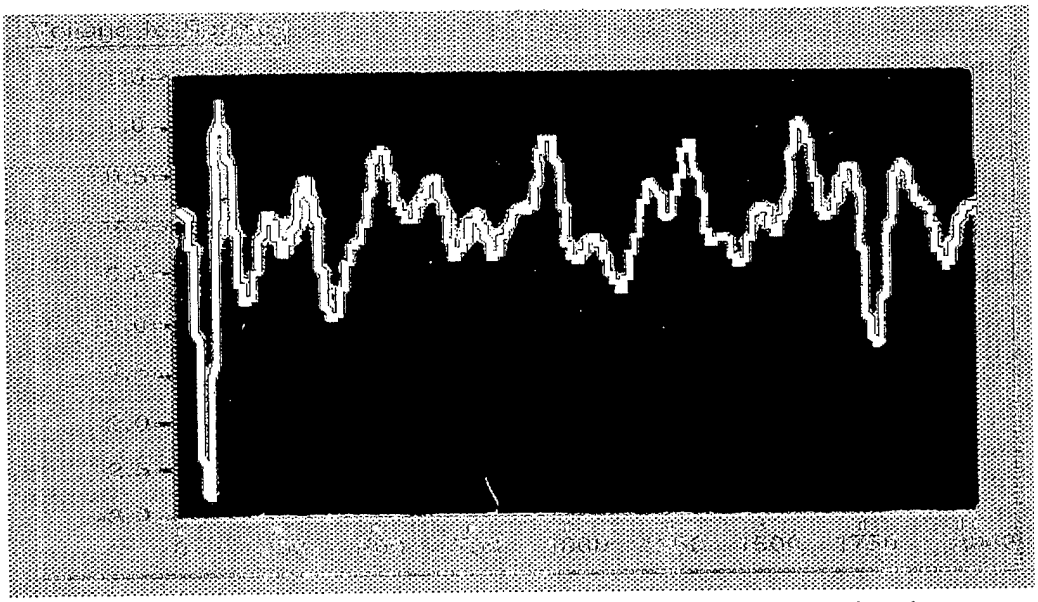

Figure 3.10. Generated voltage waveform for producing the BVI signal.

Much of the effort involved with developing the data acquisition system for the scattering experiment was in programming LabVIEW. The first virtual instrument (VI) required two analog signals to be simultaneously received by the computer. LabVIEW has some easy VI's to perform this function. The difficulty arose during the writing of the second VI, where input and output operations were needed simultaneously. LabVIEW is supposed to perform asynchronous acquisition (multiple acquisition operations at the same time). However, with the NB-A2100 board, this asynchronous acquisition did not function properly. When the program was performed step by step, it became evident that the input operation was being performed before the output. This would have been satisfactory, but the output operation did not begin until the entire input operation was complete. This created a problem because the desired BVI signal was not being acquired by the computer. The signal is present and can be displayed on an oscilloscope. Numerous attempts were made at continuous acquisition and intermediate level VI programming without success.

The following problems or potential problems still remain to be solved: the BVI signal needs to be received and digitized by the computer and circular buffering or continuous acquisition performed at higher sampling rates. Two possible solutions for receiving and digitizing the signal are to find out why LabVIEW will not perform asynchronous acquisition as advertised or install another DAQ board, one for input and the other for output. The reason circular buffering or continuous acquisition may be necessary is to prevent overloading the memory of the DAQ board at the higher sampling

frequencies of 32, 44 and 48 Khz. With long records of data and these high sampling rates, very few iterations are possible before a memory error is generated. However, the pre-distorting of the speaker signal did work. A good representation of the BVI event was seen at the microphone with an oscilloscope.

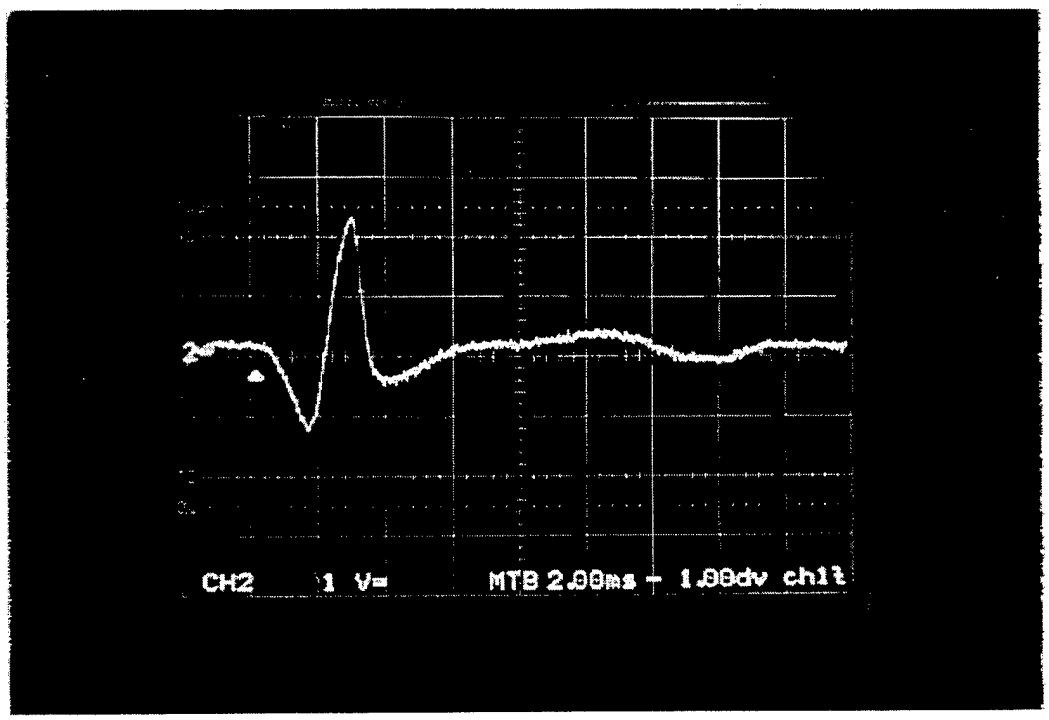


Figure 3.11. Picture of generated BVI signal taken with an oscilloscope camera.

# IV. CONCLUSIONS AND RECOMMENDATIONS

## A. SUMMARY

The objectives of the research described in this thesis were to develop a source and computer-controlled data acquisition system to generate the pressure signal that occurs during a BVI event on a model rotor blade. To accomplish this, the transfer function between the electrical signal applied to the source and the acoustic pressure measured at the leading edge of a blade hung vertically in an anechoic chamber was determined experimentally. From this transfer function was determined the desired electrical signal to be applied to the loudspeaker to generate the BVI pressure signal at the rotor blade. The resulting received signal was also digitized. Many problems were encountered, from computer compatibility problems to microphone pre-amp failure. Additionally, learning LabVIEW while trying to perform experimental measurements was quite difficult. However, the BVI signal was generated and the experiment conducted satisfactorily, allowing the scattering measurements to occur in the next phase of this research project.

## B. RECOMMENDATIONS FOR FOLLOW-ON RESEARCH

As stated previously, much research is still necessary to determine whether this is a viable alternative for initial testing of new rotor blade designs. The next phase will include determining a solution for digitizing and displaying the duplicated waveform in the computer and scattering measurements on an untreated or standard model rotor blade. These measurements will involve scattering the BVI signal off the blade and gathering

the scattered waveform for comparison with scattered data off treated blades. Due to the directionality of the radiated acoustic pressure field from a BVI event, these measurements should be taken at various angles. This would be nicely accomplished by having a stepper motor drive a microphone boom so that the angles could be known precisely.

Once the baseline scattering measurements are completed, design and testing of a treated blade will be necessary in order to verify that the scattering pattern is reduced as hypothesized. The first treated blade will be some type of Helmholtz resonator design. Once the blade is designed and manufactured, scattering measurements on this treated blade will be conducted.

If the treated blade does scatter the BVI signal less, building a full scale rotor blade of this design and testing it in a wind tunnel will be necessary in order to conclusively determine the performance of the treated blade. However, stationary scattering measurements should be a much cheaper and less time consuming way of performing initial testing of new rotor blade designs.

# APPENDIX A. EQUIPMENT SPECIFICATIONS

## A. DATA ACQUISITION BOARD NB-A2100

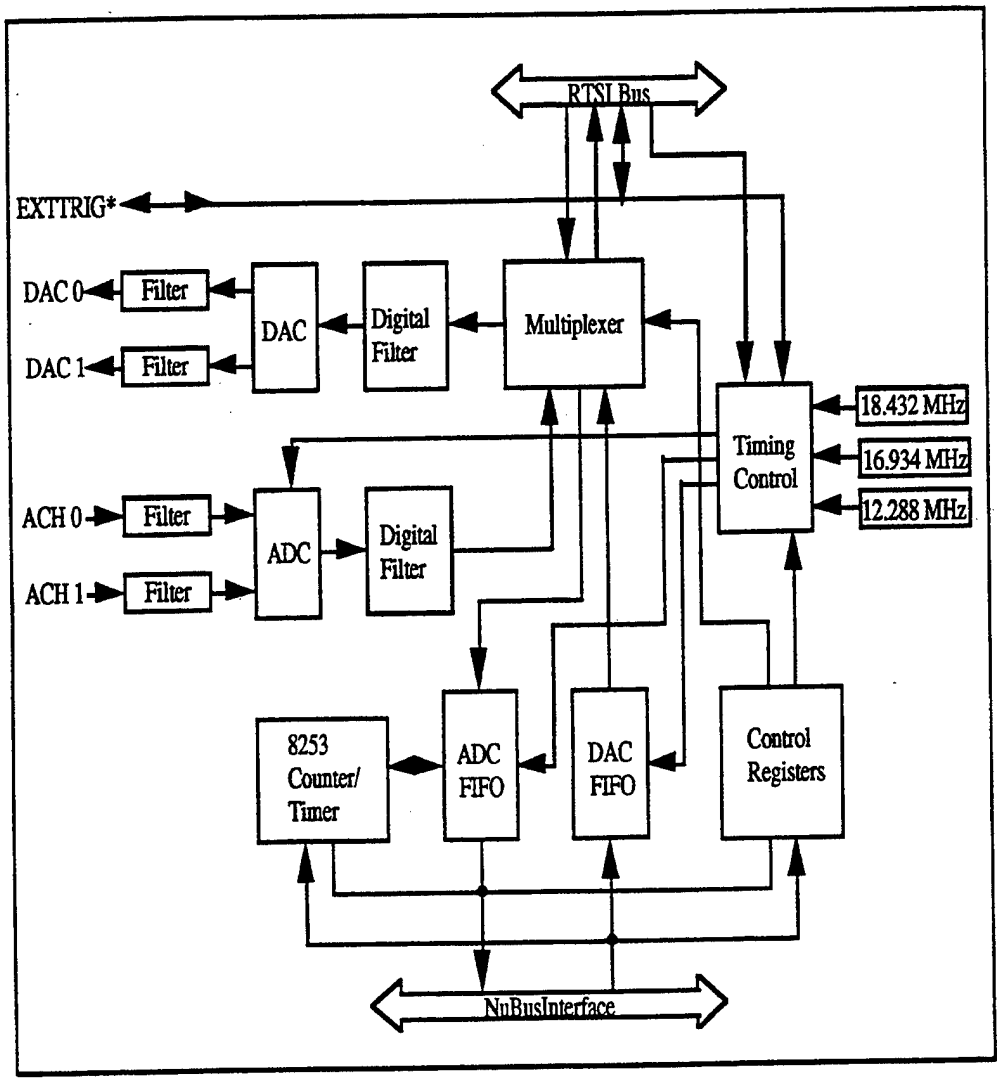


NB-A2100 high-resolution audio frequency analog I/O board.

This appendix lists the specifications of the NB-A2100 board. These specifications are typical at 25° C unless otherwise stated. The operating temperature range is 0° to 70° C.

# Analog Input

| | |
|---|---|
| Number of channels | 2, single-ended, simultaneously sampled |
| Input impedance | 470 kΩ in parallel with 220 pF |
| Input coupling | AC or DC |
| Resolution | 16 bits |
| Signal range | ±2.828 V (2 Vrms) |
| Gain adjustment range | ±3.5% (±0.25 dB) |
| Offset error (after calibration) | ±15 LSB maximum, ±5 LSB typical |
| Amplitude flatness | ±0.025 dB maximum, ±0.01 dB typical, DC to 20 kHz (48 kHz sample rate), AC coupling -3 dB cutoff at 8.8 kHz |
| Phase linearity | ±0.5°, DC to 20 kHz |
| Interchannel phase | ±1°, DC to 20 kHz |
| Total harmonic distortion (THD) | -95 dB for 0 dB input, DC to 22 kHz |
| Signal-to-THD+noise | 90 dB for 0 dB input, DC to 22 kHz |
| Intermodulation distortion (IMD), maximum harmonic products | |
| SMPTE (60 Hz, 7 kHz) | -100 dB |
| DIN (250 Hz, 8 kHz) | -100 dB |
| CCIF (14 kHz, 15 kHz) | -95 dB |
| Dynamic range (maximum signal-to-noise ratio) | 93 dB |
| Crosstalk (channel separation) | -85 dB, DC to 22 kHz |
| -3 dB bandwidth | 0.45 x sampling rate |
| Sampling rates | 22.05, 24, 32, 44.1, 48 kHz |

## Analog Output

| | |
|---|---|
| Number of channels | 2, single-ended, simultaneously sampled |
| Output impedance | 51.1 Ω |
| Output coupling | AC or DC |
| Recommended load impedance | 10 kΩ or greater |
| Resolution | 16 bits |
| Signal range | ±3 V |
| Gain error | ±6% (±0.5 dB) |
| Offset error | ±35 mV |
| Amplitude flatness | ±0.05 dB, DC to 20 kHz (48 kHz conversion rate) |
| Signal-to-THD+noise (20 Hz to 22 kHz, 0 dB output, 48 kHz conversion rate) | |
| 80 kHz bandwidth | -85 dB |
| 20 kHz bandwidth | -90 dB |
| Intermodulation distortion (IMD), maximum harmonic products | |
| CCIF (14 kHz, 15 kHz) | -90 dB |
| Dynamic range (maximum signal-to-noise ratio) | 92 dB |
| Crosstalk (channel separation) | -95 dB, DC to 22 kHz |
| -3 dB bandwidth | 0.50 x conversion rate |
| Conversion rates | 16, 22.05, 24, 32, 44.1, 48 kHz |

## Digital Trigger

| | |
|---|---|
| Input level | TTL-compatible |
| Response | Falling edge |
| Minimum pulse width | 50 nsec |
| Output level | TTL-compatible |
| High-level output current | -8.0 mA |
| Low-level output current | 8.0 mA |

## RTSI

| | |
|---|---|
| Trigger | 1 |
| DMA Channels | 2 |
| Serial Link | 2 full-duplex serial links capable of transfer rates up to 1.536 Mbits/sec |

## Power Requirement (from NuBus)

| | |
|---|---|
| Power consumption | 1.75 A at +5 VDC |

## Physical Characteristics

| | |
|---|---|
| Board dimensions | 12.875 in. x 4 in. |
| I/O connector | 5 RCA-type phono jacks |

## Operating Environment

| | |
|---|---|
| Component temperature | 0° to 70° C |
| Relative humidity | 5% to 90% noncondensing |

## Storage Environment

| | |
|---|---|
| Temperature | -55° to 150° C |
| Relative humidity | 5% to 90% noncondensing |

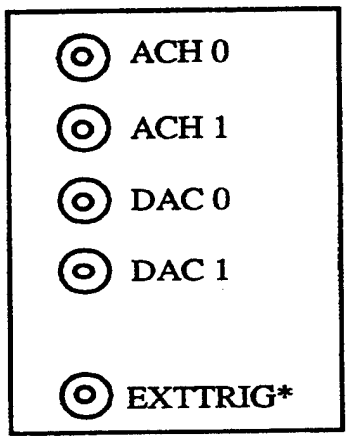


ACH 0 and ACH 1 are analog input channels and DAC 0 and DAC 1 are analog output channels

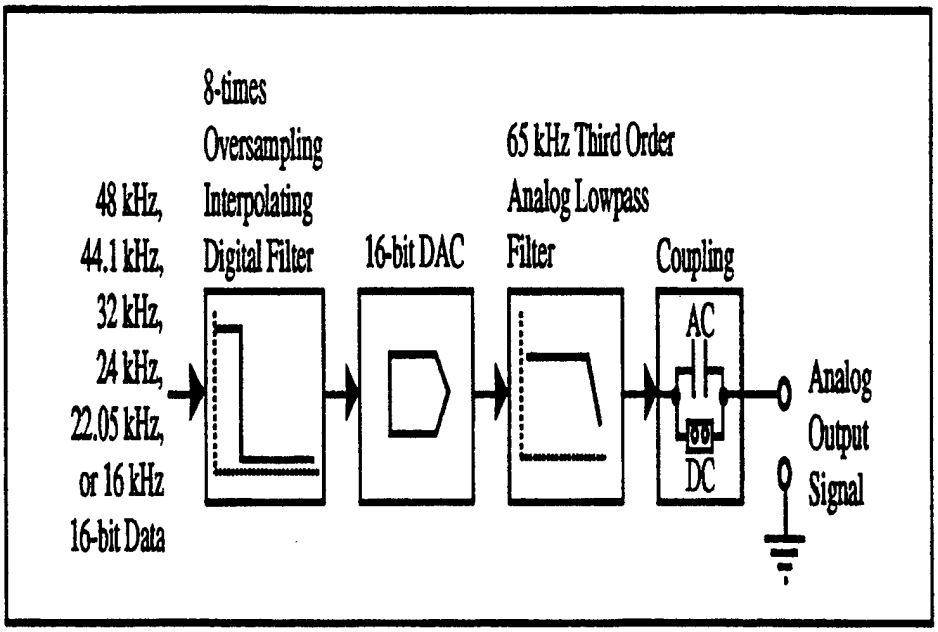


NB-A2100 analog output circuitry

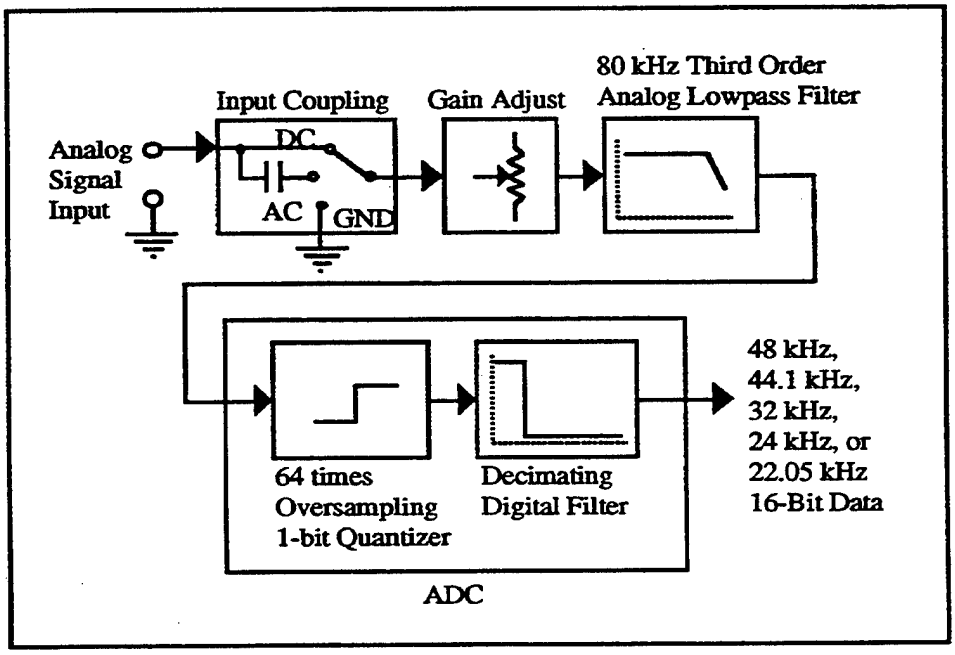


NB-A2100 analog input circuitry

# APPENDIX B. ITHACO LOW NOISE PRE-AMP SPECIFICATIONS

IPS-134

## MODEL 1201
## LOW NOISE
## PROGRAMMABLE PREAMPLIFIER

**ITHACO**

735 WEST CLINTON STREET, ITHACA, NEW YORK 14850, PHONE 607-272-7640, TWX 510-255-9307

### SPECIFICATIONS

| | |
|---|---|
| INPUT IMPEDANCE | DC Coupled: Greater than 1 gigohm (1000 megohms); typically 5 gigohms (5000 megohms).<br>AC Coupled: 100 megohms |
| INPUT CURRENT | Less than 10pA, either input; less than 5pA difference (offset) current. |
| INPUT FREQUENCY RESPONSE | < 0.008 Hz (AC coupled) |
| DC STABILITY (vs. Temperature) | 6μV/°C max, referred to input; 300μV/°C max, referred to output. |
| DC STABILITY (vs. Time) | 20μV/24 hr, non-cumulative, maximum, after ½ hour warmup. |
| MAXIMUM INPUT, COMMON MODE | 10 volts, pk-pk, minimum. |
| MAXIMUM INPUT, DIFFERENTIAL OR SINGLE-ENDED | ±750mV (gains of X10 – X100)<br>±75mV (gains of X200 – X10K) |
| COMMON MODE REJECTION (Minimum) | Frequency / Gain > 200 / Gain < 200<br>DC – 100 Hz: 125 dB / 115 dB<br>1 kHz: 105 dB / 95 dB<br>10 kHz: 85 dB / 75 dB<br>100 kHz: 65 dB / 55 dB<br>200 kHz: 55 dB / 45 dB<br>400 kHz: 50 dB / 40 dB |
| GAIN | X10 to X10,000 in a 1-2-5-10 sequence; front panel potentiometer provides continuous gain to X25,000. |
| GAIN ACCURACY | Better than 1% when vernier is in CAL position. |
| GAIN STABILITY | Better than 0.03%/°C. |
| DISTORTION | Typically less than 0.01%. |
| FREQUENCY RESPONSE | DC Coupled: DC to 400 kHz (–3 dB) with low pass switch in MAX position.<br>AC Coupled: 0.008 Hz to 400 kHz (–3 dB) with low pass switch in MAX position. |
| HIGH PASS FILTER (low frequency rolloff) | Switch-selectable from DC and 0.03 Hz to 3 kHz, in a 1-3-10 sequence. |
| LOW PASS FILTER (high frequency rolloff) | Switch-selectable from 3 Hz to 300 kHz and MAX in a 1-3-10 sequence; bandwidth in MAX position is 400 kHz minimum. |
| NOISE FIGURE | Less than 0.4 dB at 10 Hz, with a 1 megohm source impedance.<br>Less than 0.04 dB at 1 kHz, with a 1 megohm source impedance. |
| NOISE | Less than 15 nV per Hz $^{-½}$ at 10 Hz.<br>Less than 7 nV per Hz $^{-½}$ at 1 kHz. |
| OUTPUTS | Four outputs (BNC) as follows: a) 600Ω outputs (2). b) Lo-Z output (to 25 mA, 50 Ω). c) Unity-gain (X1) output. |
| MAXIMUM OUTPUT VOLTAGE (battery operation) | a) 600Ω outputs: 12 volts pk-pk, minimum.<br>b) Lo-Z output: 10 volts pk-pk minimum, up to 25 mA.<br>c) Unity-gain (X1) output: 1.3 volts pk-pk minimum, up to 7 mA. |
| MAXIMUM OUTPUT VOLTAGE (line operation) | a) 600Ω outputs: 20 volts pk-pk, minimum.<br>b) Lo-Z output: 18 volts pk-pk minimum, up to 25 mA.<br>c) Unity-gain (X1) output: 2 volts pk-pk, minimum, up to 7 mA. |
| GATED OPERATION | Preamplifier may be gated with external input (rear panel BNC). Any waveform type, including TTL or contact closure, is permissable. Minimum duration (pulse) is 20μsec. |
| REMOTE PROGRAMMING | Option (user-installable) inputs permit remote control of gain (from X10 to X10,000 in a 1-2-5-10 sequence), overload recovery and gating. Gain and/or overload may be latched. Device select function line allows multiplexing several Model 1201 Preamplifiers.<br>Option outputs indicate remote operation, incorrect gain command, gain status, gain un-CAL, overload, low pass filter status and high pass filter status. Format is BCD-coded. |

## APPENDIX C. PIONEER SPEAKER SPECIFICATIONS

**PIONEER®**

**1½" Soft Dome Midrange**

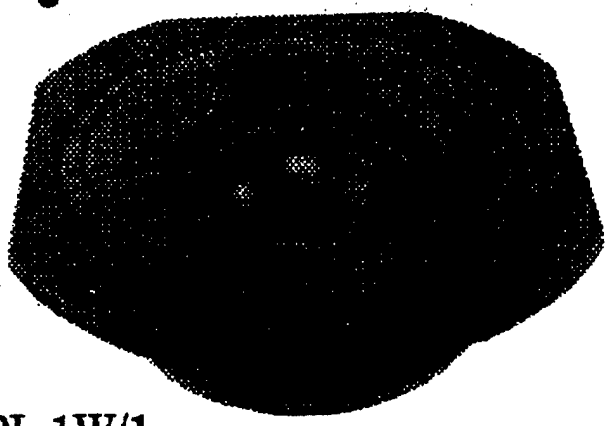

•Ferrofluid cooled and closed backed for optimum performance •Ferrite magnet: 7.2 oz. •Voice coil: 1½" •6.5ohm •Power handling: RMS/peak 30/60W •Sensitivity SPL 1W/1 meter: 92dB •Frequency response: 1.2KHz~15KHz •Mounting dimensions: 3$\frac{1}{16}$" x 3$\frac{1}{8}$"

## APPENDIX D. ANECHOIC CHAMBER

The anechoic chamber provides an echo-free region for conducting basic acoustic research. It is advantageous because it contains low external noise due to its floating room within a room concept. It is build with concrete and fiberglass. The 40 inch fiberglass wedges are designed to absorb 99% of the energy above 100 cycles/sec and they occupy a volume of 5000 cubic feet. The floor consists of 225 wire cables each stretched to a tension between 150 and 200 pounds. The working dimensions of the chamber are 27' X 14' X 11'.

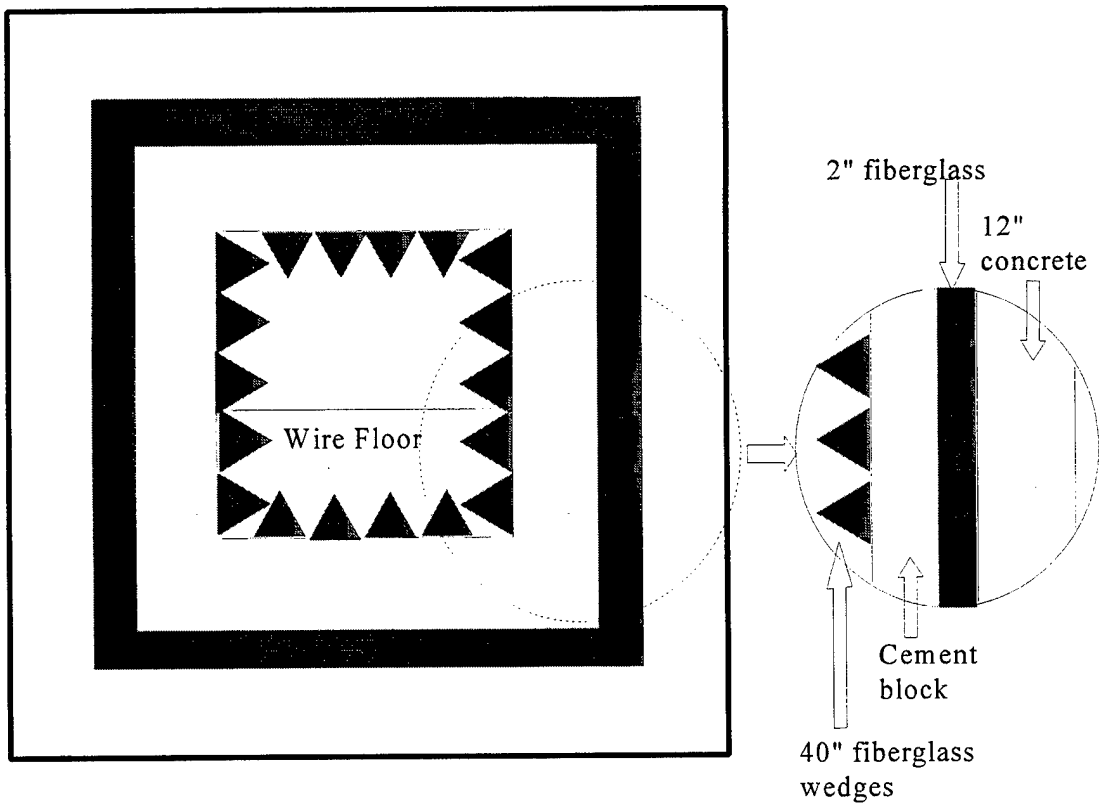

## APPENDIX E. LABVIEW COMPUTER CODE

The front panels and block diagrams for both virtual instruments (VI) along with a brief description and some component information are shown.

This VI determines the transfer fucntion of a given device. It is used in conjunction with BVI1.VI for producing a given signal at a microphone. It was designed specifically for determining the transfer fucntion of a rotor blade for Brian Roth's masters thesis in December 1996. However, it will determine the transfer function of any device.

Before using this VI, a noise source needs to be used and sent both to a speaker in the anechoic chamber and to analog input channel 0 of the DAQ board. Additionally, the microphone output has to be connected to analog input channel 1. The VI is run by simply turning on the power and depressing the run arrow. When a sufficient amount of data has been taken, the VI is stopped by turning off the power. The VI produces the average impulse response, magnitude and phase, along with the average transfer function, magnitude and phase. Additionally, it gives a continues display of the tranfer function of each iteration.

**********NOTE**********

This VI must be run each time before running BVI1.VI to ensure the proper transfer fucntion has been determined for the specific acoustic conditions existing inside the anechoic chamber.

---

**Samples**

The number of samples taken each time a sample is conducted. If keep this number a power of two, labview uses quich FFT algorithm.

**Channels**

Analog input channels that are being sampled. Channel 0 corresponds to the noise and channel 1 to the microphone.

**Output file name**

Output file where the magnitude and phase of the transfer function are stored.

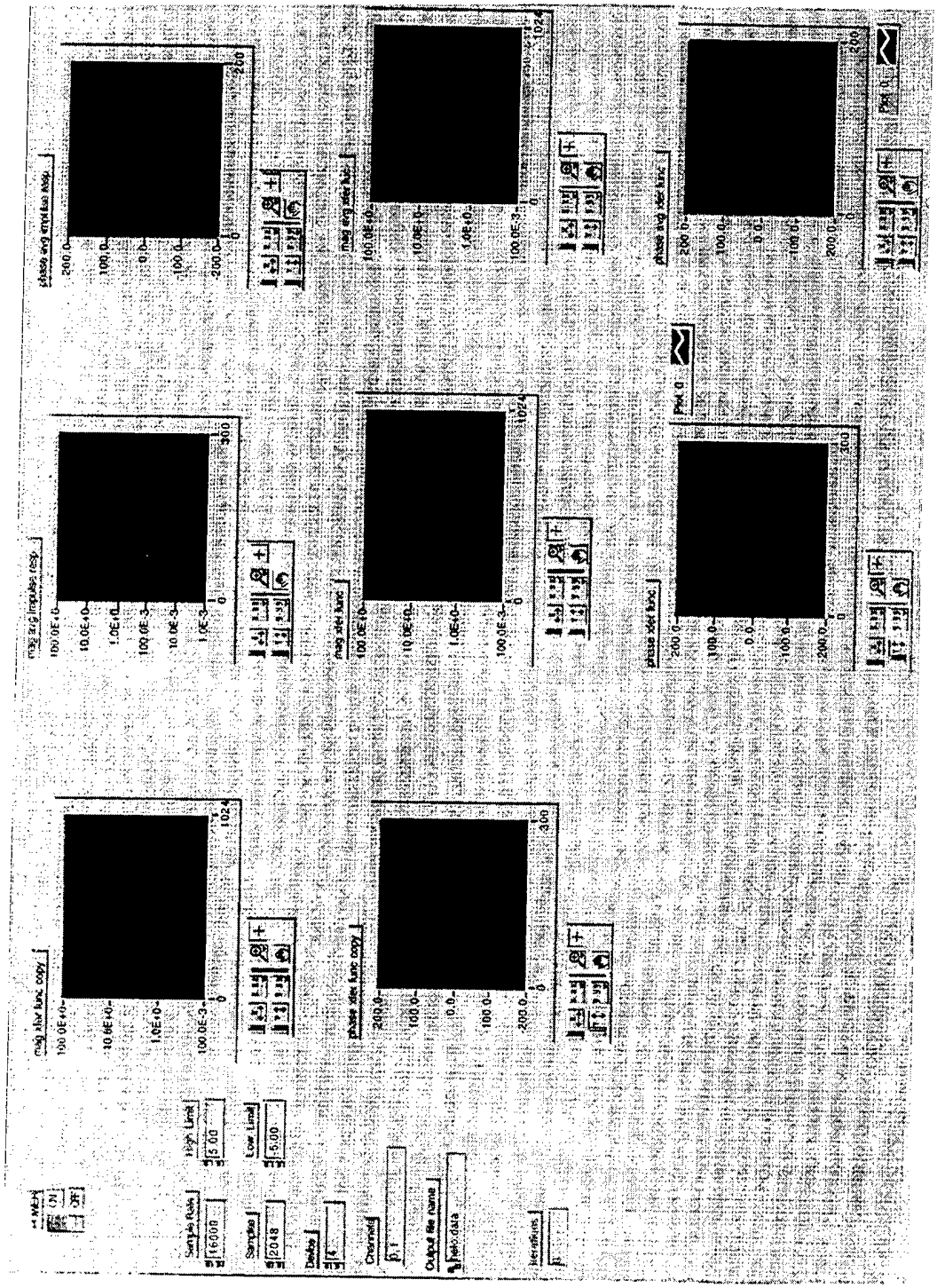


Front panel for transfer function VI

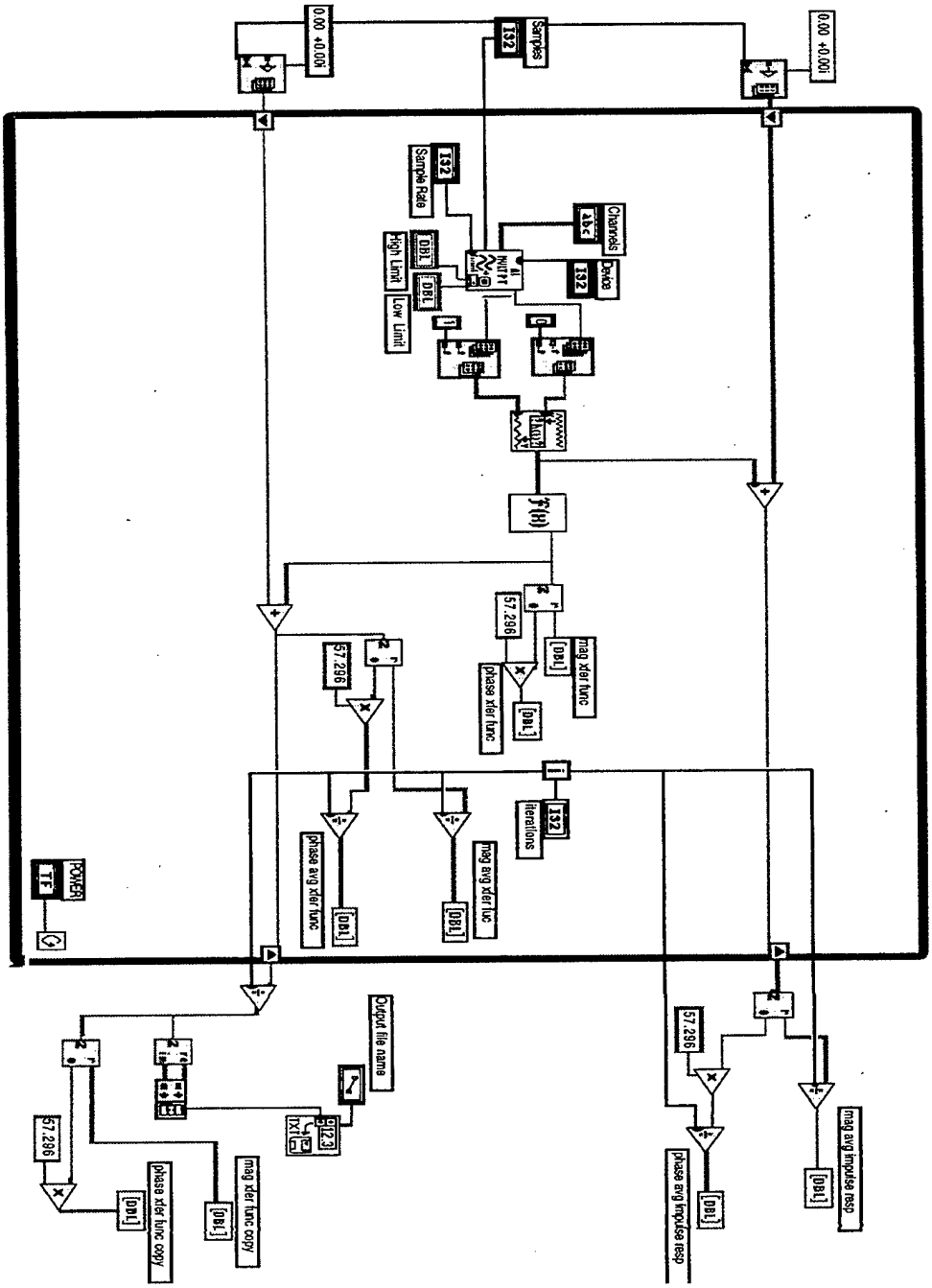


Diagram for transfer function VI

**BVI**
File where the desired BVI signal is stored

**Transfer function**
File where the transfer function magnitude and phase are stored

**Device**
Device number of NB-A2100 DAQ board

**Channel**
Analog output channel where voltage is sent to speaker and analog input channel collecting the signal from the

**update rate**
Rate at which the voltage is generated and BVI signal is sampled

**POWER**

**Amplitude**
Amplitude of the output voltage

**Final amp**
Amplitude of the final or generated BVI event

**samples**
Number of samples collected per scan

**Voltage to Speaker**

**Desired BVI**

**Stored Transfer Function mag**

**BVI Final**

**Stored Transfer Function phase**

Description of the VI for determining and storing the system transfer function.

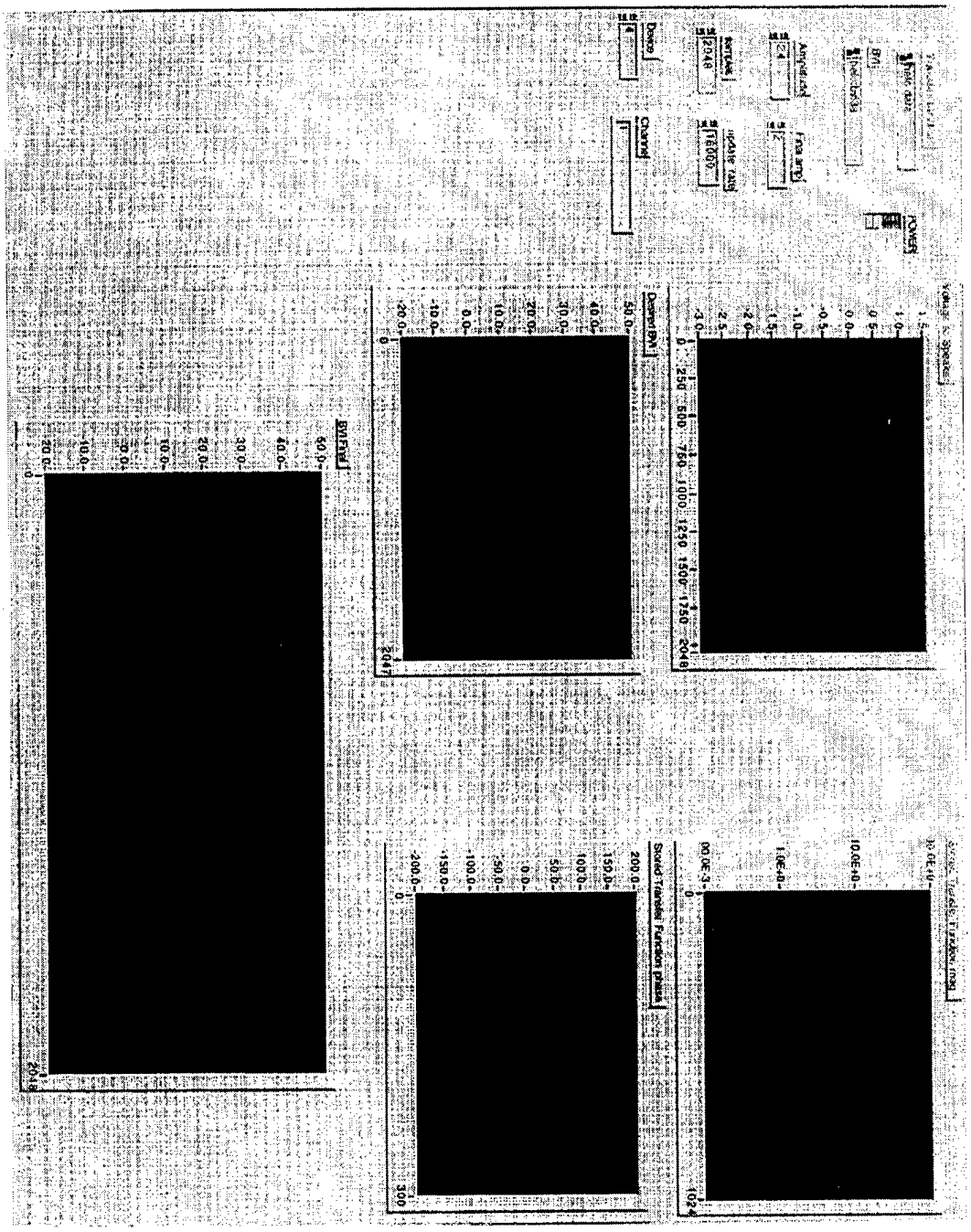

Front panel for BVI signal generation VI

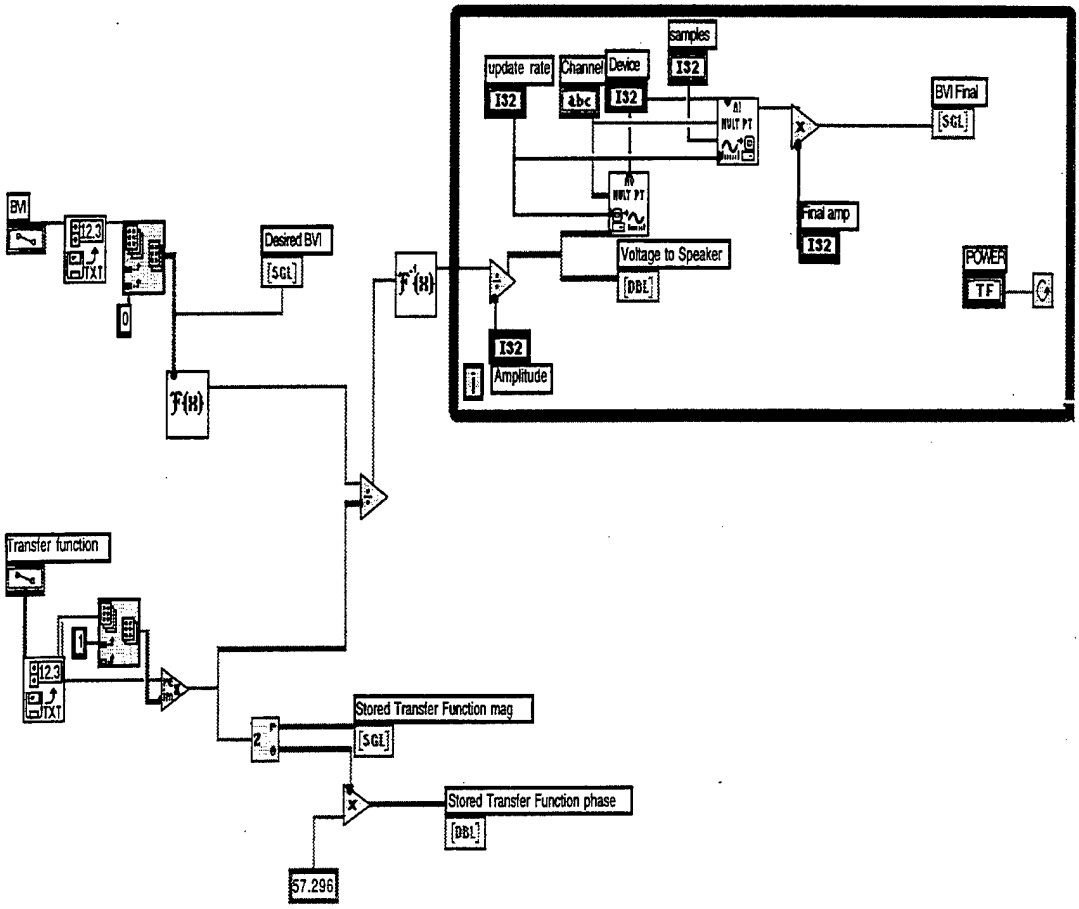


Diagram for generating desired BVI signal

## LIST OF REFERENCES


Brooks, T.F., "Studies of Blade-Vortex Interaction Noise Reduction By Rotor Blade Modification", Noise-Con 93, pp 57-66, 1993.

El-Ghobashy, N., Visualization of Helicopter/Tiltrotor Blade-Vortex Interaction, 1996.

George, A.R., "Helicopter Noise: State-of-the-Art", J. Aircraft vol 15, no. 11, pp 707-715, 1978.

Hawkings, D. L. and Lowson, M. V., "Theory of Open Supersonic Rotor Noise", Journal of Sound and Vibration vol. 36 no. pp. 1-8, 1974.

Hubbard, H.H., *Aeroacoustics of Flight Vehicles, Theory and Practice Volume 1: Noise Sources*, pp 65-149, Acoustical Society of America, 1995.

Kinsler, L.E., Frey, A.R., Coppens, A.B., and Sanders, J.V., *Fundamentals of Acoustics, Third Edition*, pp. 258-259, John Wiley & Sons, 1982.

National Instruments, 1996, 6504 Bridge Point Parkway, Austin, TX 78730-5039, (800) 433-3488.

Pioneer Electronic Corporation of America (speakers were purchased through MCM Electronics), 1996, (800) 457-2881

Proakis, J.G. and Manolakis, D.G., *Digital Signal Processing Principles, Algorithms, an d Applications* second edition, pp 75-77, 185, Macmillian Publishing Company, 1992.

Schmitz, F.H. and Yu, Y.H., "Helicopter Impulsive Noise: Theoretical and Experimental Status", Journal of Sound and Vibration vol. 109, no. 3, pp. 361-422, 1986.

Sim, B.W. and George, A.R., "Development of a Rotor Aerodynamic Load Prediction Scheme for Blade-Vortex Interaction Noise Study," American Helicopter Society 51st Annual National Forum, Fort Worth, Texas, pp 525-546, May 1995.

## INITIAL DISTRIBUTION LIST

| | No. Copies |
|---|---|
| 1. Defense Technical Information Center<br>8725 John J. Kingman Rd., STE 0944<br>Ft. Belvoir, VA 22060-6218 | 2 |
| 2. Dudley Knox Library<br>Naval Postgraduate School<br>411 Dyer Rd.<br>Monterey, CA 93943-5101 | 2 |
| 3. Professor Steven R. Baker<br>Department of Physics, Code PH/Ba<br>Naval Postgraduate School<br>Monterey, California 93943-5103<br>(408) 656-2732 | 1 |
| 4. Professor Robert M. Keolian<br>Department of Physics, Code PH/Kn<br>Naval Postgraduate School<br>Monterey, California 93943-5103<br>(408) 656-2232 | 1 |
| 5. Professor E. Roberts Wood<br>Department of Aeronautical Engineering, Code AA/Wd<br>Naval Postgraduate School<br>Monterey, California 93943-5103<br>(408) 656-2897 | 1 |
| 6. Professor Joshua Gordis<br>Department of Mechanical Engineering, Code ME/Go<br>Naval Postgraduate School<br>Monterey, California 93943-5103<br>(408) 656-2866 | 1 |
| 7. Professor Don Danielson<br>Department of Mathematics, Code MA/Da<br>Naval Postgraduate School<br>Monterey, California 93943-5103<br>(408) 656-2622 | 1 |

8. LT Brian D. Roth
510 Reade Avenue
Upland, IN 46989

2